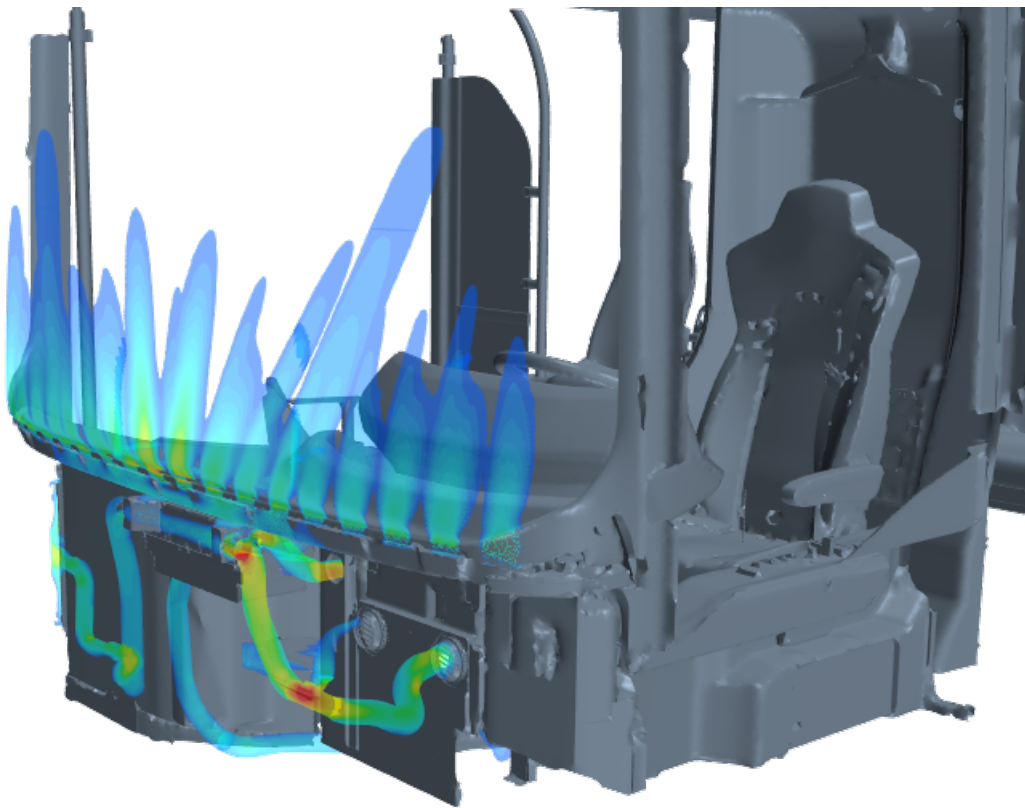




**CHALMERS**  
UNIVERSITY OF TECHNOLOGY

---



# **Interior climate simulation of electric buses**

Master thesis in Applied Mechanics

Edvin Eriksson Johansson  
Maja Skärby



MASTER THESIS 2019:31

# Interior climate simulation of electric buses

EDVIN ERIKSSON JOHANSSON  
MAJA SKÄRBY



**CHALMERS**  
UNIVERSITY OF TECHNOLOGY

Department of Mechanics and Maritime Sciences  
*Division of Vehicle Engineering and Autonomous System*  
CHALMERS UNIVERSITY OF TECHNOLOGY  
Gothenburg, Sweden 2019

Interior climate simulation of electric buses  
EDVIN ERIKSSON JOHANSSON  
MAJA SKÄRBY

© EDVIN ERIKSSON JOHANSSON, MAJA SKÄRBY 2019.

Supervisor: Raman Yazdani, Volvo Bussar AB  
Examiner: Simone Sebben, Division of Vehicle Engineering and Autonomous System

Master Thesis 2019:31  
Department of Mechanics and Maritime Sciences  
Division of Vehicle Engineering and Autonomous System  
Chalmers University of Technology  
SE-412 96 Gothenburg  
Sweden  
Telephone +46 (0)31-772 1000

Cover: Visualization of air blowing on the windscreen and driver simulated in star CCM+.

Chalmers Reproservice  
Gothenburg, Sweden 2019

Interior Climate Simulation of Electric Buses  
EDVIN ERIKSSON JOHANSSON  
MAJA SKÄRBY  
Department of Mechanics and Maritime Sciences  
Chalmers University of Technology

## **Abstract**

Today a large part of the power consumption for public transport vehicles is used by the Heat, Ventilation and Air Conditioning, HVAC, system to ensure climate comfort in the bus. In the transition to electrical vehicles it is of high importance to reduce the HVAC systems power consumption. With electrical vehicles the power consumption for the HVAC system is competing with the driving range for the vehicle since there is a limited battery capacity. By simulating the interior climate in buses investigations on how to reduce the power consumption of the HVAC system can be done. Simulations enable that more parameters can be tested compared with experimental testing.

In this master thesis a first draw of a method for simulating interior climate has been developed. The method is based on CFD analyze of flow and temperature in steady state. No passengers are included in the simulation and passengers comfort are not taken into account. Important findings regarding meshing, boundary conditions and physics models for the numerical CFD analysis are presented. A heat transfer coefficient, HTC, sweep has been performed to calibrate the simulation model to experimental data.

Keywords: Electric buses, interior climate, numerical simulation, HVAC, CFD



## **Preface**

This master's thesis has been performed during the spring of 2019 by Edvin Eriksson Johansson and Maja Skärby as a part of the master's program Applied Mechanics at Chalmers University of Technology. The thesis was performed at Volvo Bus Corporation and supervised by Raman Yazdani (Lead simulation engineer, fluid dynamics) and examined by Prof. Simone Sebben at Division of Mechanics and Maritime Sciences at Chalmers University of Technology.

## **Acknowledgements**

We would like to thank our excellent supervisor Raman Yazdani for his genuine support in this project. His help and guidelines have been very beneficial in pushing this project forward in the right direction. We would also like to thank the people at the Virtual Verification & Analysis department for letting us feel welcome and for further help with specific software issues. From Chalmers University of Technology we would like to thank Simone Sebben for being our examiner.



---

## Abbreviations

<b>CFD</b>	Computational Fluid Dynamics
<b>HVAC</b>	Heat, Ventilation, Air Condition
<b>AC</b>	Air Condition
<b>HTC</b>	Heat Transfer Coefficient

## Nomenclature

$x_i$	Location in i-direction
$v_i$	Velocity in i-direction
$t$	Time
$\rho$	Density
$\phi$	Viscous dissipation
$\sigma_{ij}$	Stress tensor
$\tau_{ij}$	Reynolds stress tensor
$\kappa$	Conductivity constant
$\mu$	Viscosity
$c_p$	Specific heat constant
$T$	Temperature
$k$	Turbulent kinetic energy
$\varepsilon$	Turbulent dissipation rate
$l$	Turbulent length scale
$C_\mu$	Constant for k- $\varepsilon$ models
$Y_+$	Dimensionless wall distance
$h$	Convection heat transfer coefficient
$q''$	Convective heat flux
$\sigma_B$	Boltzmann constant
$E$	Total energy
$Q$	Heat transfer
$W$	Work
$\dot{m}$	Mass flow rate
$\dot{V}$	Volume flow rate



# Contents

<b>Abbreviations</b>	<b>ix</b>
<b>1 Introduction</b>	<b>1</b>
1.1 Background . . . . .	1
1.2 Aim and purpose . . . . .	1
1.3 Delimitations . . . . .	2
1.4 Objective . . . . .	2
1.5 Ethical considerations . . . . .	2
<b>2 Theory</b>	<b>5</b>
2.1 Governing equations . . . . .	5
2.2 Turbulence model . . . . .	6
2.3 Heat transfer . . . . .	6
2.3.1 Convection . . . . .	7
2.3.2 Radiation . . . . .	7
2.3.3 Heat transfer rate . . . . .	7
<b>3 Method development</b>	<b>9</b>
3.1 Components in the HVAC system . . . . .	9
3.2 Mesh construction . . . . .	10
3.2.1 Surface Wrapper . . . . .	11
3.2.2 Volume mesh generation . . . . .	13
3.3 Simulating physics and solver settings . . . . .	16
3.3.1 Physics models . . . . .	16
3.3.2 Solver settings . . . . .	19
3.4 Boundary Conditions . . . . .	19
3.5 Model calibration with experimental data . . . . .	23
3.5.1 Collection of experimental data . . . . .	23
3.5.2 HTC sweep . . . . .	24
3.6 Summation of method development findings . . . . .	24
<b>4 Results and discussion</b>	<b>27</b>
4.1 Physics Simulation . . . . .	27
4.1.1 Convergence . . . . .	27
4.1.2 Flow shape . . . . .	29
4.1.3 Temperature fields . . . . .	31
4.1.4 Boundary heat flux . . . . .	32

## Contents

---

4.2	HTC calibration sweep . . . . .	35
4.2.1	Warm case . . . . .	35
4.2.2	Cold case . . . . .	39
4.2.3	Comparison between cases results . . . . .	43
<b>5</b>	<b>Conclusion</b>	<b>45</b>
5.1	Future Work . . . . .	46
	<b>Bibliography</b>	<b>47</b>

# 1

## Introduction

This chapter gives an introduction to the master thesis work. The background explains the importance of the topic, after that the aim and purpose of the thesis is stated. This is followed by a description of the limitations and more detailed objectives. The chapter is finished with ethical considerations.

### 1.1 Background

Today a large part of the power consumption for public transport vehicles is used by the Heat, Ventilation and Air Conditioning, HVAC, system [1]. Especially the power consumption is large in extreme weather conditions when the outdoor climate is very hot and humid or when it is cold [2]. It is extra important in the transition to electrical vehicles to use the HVAC system effectively to adjust the interior climate because of the limited battery capacity as well as for attracting more people to use public transport systems [3].

It is expensive and time consuming to produce real world tests on buses [4]. In the same time experiments are limited to a smaller range of test settings that can also be hard to produce. Simulating the interior can therefore both improve efficiency and be used to save costs.

By improving the performance of HVAC systems, less energy can be used for cooling and heating and in that way increase the range for electric buses without impairing the comfort of passengers and the driver[2][5]. Optimal energy consumption and interior climate quality can be achieved by simulating the interior of the vehicle together with the climate system. Numerical CFD simulations enhance the possibility to find details that are not possible to discover in experiments, thus it is helpful for optimizing energy usage of the HVAC system. Tests can still be used to verify the simulation results in real world conditions to ensure customer satisfaction.

### 1.2 Aim and purpose

The aim is to develop a methodology for Volvo Buses of how to simulate the interior climate in different bus models. This developed method can be used to investigate the interior climate in a bus and give recommendations on how to improve it. The goal is to minimize energy consumption without impairing the driver and passenger climate experience.

### 1.3 Delimitations

To be able to develop a method for simulating interior climate some simplifications have to be made due to limited time resource of 20 weeks and computer capacity. The simplifications are listed as:

- Simulate the Air Conditioning (AC) unit and heat pump system on the roof as a one dimensional black box with added effect.
- Simulate the defroster in the front also as a black box.
- Air stream coming out from the system is based on manufacturer volume flow data.
- Only the interior airflow and temperature will be investigated.
- Only investigate steady state cases.
- No passengers included in the simulations since there are experiments available without passengers.
- Investigation of passenger and driver climate comfort is not included.

The limited computer capacity leads to slower work flow when working in simulation programs. It also limits the refinement grade and the number of configurations tested. Learning two new softwares have also been a time restriction. It is important to clarify that this is a first step in developing a method for simulating interior climate and not a final method.

### 1.4 Objective

To structure the work in the thesis the project is divided into subtasks. Each subtask is a question that should be answered to fulfill the aim of the project. The following objectives were chosen to be critical in this method development:

- What parts and components are important to bring into a CFD model for the interior climate?
- How should the mesh strategy be applied for convergence and reliable results?
- What needs to be known about the HVAC system to get the right boundary conditions?
- Which settings are important for a numerical Computational Fluid Dynamics (CFD) analysis of the interior climate?
- What models for turbulence should be used for reliable results?
- How does the flow field and temperature change for different HVAC system configurations?
- How does the interior climate change depending on the outdoor temperature?
- How can the model be calibrated with experimental data?

### 1.5 Ethical considerations

A method that can simulate the interior climate will help the development of electrical buses and ensure comfortable interior climate. This can enhance a safe work environment for bus drivers and the improved passenger comfort will hopefully increase the usage of public transportation.

A more efficient use of the HVAC system can also increase the driving range of the buses. With longer driving range electrical buses can compete against traditional options with combustion engines. This can have positive effects on the climate and reduce the amount of CO<sub>2</sub> emissions. This goes well in line with UN:s sustainable development goals, especially goal 11 "Sustainable Cities and Communities" and goal 13 "Climate Action"[6].



# 2

## Theory

In this section, theory that might be good for increasing the understanding of the report will be presented. The governing equations for fluid flow and heat transfer are described together with the chosen turbulence model. There is also a section about heat transfer which includes convection, radiation and heat transfer rate.

### 2.1 Governing equations

For fluid flow and heat transfer there are three governing equations: the continuity equation (mass conservation), the momentum equation and the energy equation.

**The continuity equation** is

$$\frac{d\rho}{dt} + \rho \frac{\partial v_i}{\partial x_i} = 0 \quad (2.1)$$

where  $\rho$  is the fluids density,  $t$  is the time,  $x_i$  is the location and  $v_i$  is the velocity in the  $i$ -direction. For incompressible flow the density is constant and the continuity equation can be written as:

$$\frac{\partial v_i}{\partial x_i} = 0 \quad (2.2)$$

**The momentum equation** states according to Newtons second law that the rate of change of the momentum of a fluid particle is equal to the sum of the forces on the fluid particle:

$$\rho \frac{dv_i}{dt} = \frac{\partial \sigma_{ji}}{\partial x_j} + \rho f_i \quad (2.3)$$

where  $\sigma_{ij}$  is the stress tensor and  $f_i$  are the volume forces. For a newtonian viscous fluid the stress tensor can be written as

$$\begin{aligned} \sigma_{ij} &= -P\delta_{ij} + 2\mu S_{ij} - \frac{2}{3}\mu S_{kk}\delta_{ij}, \\ \tau_{ij} &= 2\mu S_{ij} - \frac{2}{3}\mu S_{kk}\delta_{ij} \end{aligned} \quad (2.4)$$

Inserting Eq. 2.4 in Eq. 2.3 and assuming incompressible flow and constant viscosity,  $\mu$ , gives the momentum equation

$$\rho \frac{dv_i}{dt} = -\frac{\partial P}{\partial x_i} + \mu \frac{\partial^2 v_i}{\partial x_j \partial x_j} + \rho f_i \quad (2.5)$$

In the first law of thermodynamics it is stated that the rate of change of energy of a fluid particle is equal to the rate of heat addition to the fluid particle plus the rate of work done on the particle. For an incompressible fluid **the energy equation** can be written as

$$\rho c_p \frac{dT}{dt} = \Phi + \frac{\partial}{\partial x_i} \left( \kappa \frac{\partial T}{\partial x_i} \right) + \rho z \quad (2.6)$$

where the term on the left side defines the internal energy with the specific heat capacity,  $c_p$ , and temperature,  $T$ . On the right hand side  $\Phi$  defines the viscous dissipation, the second term is the heat flux with the thermal conductivity constant,  $\kappa$ , and the last term on right hand side is the net radiative heat source [7][8].

## 2.2 Turbulence model

Turbulent flow is modelled with wall functions close to the walls which allows the first node to be located further away from the wall and thus allow a coarser grid saving computational power. The used **Realizable Two-Layer k-epsilon** model solves modelled transport equations for  $k$  and  $\varepsilon$ . The turbulent length scale comes from

$$l = \frac{k^{2/3}}{\varepsilon} \quad (2.7)$$

and the turbulent viscosity comes from

$$\nu_t = c_\mu k^{1/2} l = c_\mu \frac{K^2}{\varepsilon} \quad (2.8)$$

Compared with the standard  $k - \varepsilon$  model the term **Realizable** means the model contains a new transport equation for the turbulent dissipation rate and one of the previous constants,  $c_\mu$ , is expressed as a function of turbulent properties and mean flow instead of assumed to be constant. This will let the model to fulfill mathematical constraints on the normal stresses[7]. The realizable model is typically better at simulating three dimensional flow around complex geometries[9].

The term **Two-Layer** means that the turbulent dissipation rate  $\varepsilon$  and the turbulent viscosity  $\mu_t$  are functions depending on wall distance in flow regions close to walls. This means that the flow is treated in two different ways depending on the distance to the closest wall. The modelled values are blended smoothly with the values computed from solving the corresponding transport equations far away from the walls. In total, the used model can be used for a larger extent of  $Y^+$  values[9].

## 2.3 Heat transfer

An important part of the simulation will be the heat transfer, both within the fluid and between the fluid and solid surfaces. This section describes some theory of heat transfer.

### 2.3.1 Convection

Convection is used to describe heat transfer between a fluid and a surface. In the term convection the energy is transported both by the bulk fluid motion (advection) as well as the random motion of fluid molecules (conduction or diffusion). The conduction heat rate  $q_{cond}$  can be described by the heat flux over an area as

$$q_{cond} = -\kappa A \frac{dT}{dx} \quad (2.9)$$

There are two types of convection, natural and forced. **Natural convection** is due to buoyancy forces i.e. due to density differences caused by differences in temperature. In **forced convection** the movement is induced by external means e.g. a fan or pump. This results in larger temperature and velocity gradients in the boundary layer. Forced convection is used for enhancing heating or cooling. The convective heat flux can be described as

$$q'' = h(T_s - T_f) \quad (2.10)$$

where  $h$  is the convection heat transfer coefficient.  $T_s$  and  $T_f$  are the temperatures on the surface and in the fluid respectively[10].

### 2.3.2 Radiation

Thermal radiation is heat emitted by all bodies with a temperature greater than absolute zero. The maximum emission is from a so called black body according to Boltzmann law

$$q''_{bb} = \sigma_B T_s^4 \quad (2.11)$$

where  $T_s$  is the surface temperature and  $\sigma_B$  is the Boltzmann constant. A real surface is emitting a heat flux less than that of an ideal black body. Therefore the heat flux is calculated as

$$q''_{rad} = \varepsilon \sigma_B T_s^4 \quad (2.12)$$

where  $0 \leq \varepsilon \leq 1$  is the surface emissivity, specific for each surface.

### 2.3.3 Heat transfer rate

The total heat energy rate going into a closed system is calculated by using energy balance. The energy balance comes from the first law of thermodynamics as

$$\Delta E = Q + W \quad (2.13)$$

where  $E$  is the total energy,  $W$  is the work done on the system and  $Q$  is the heat transfer into the system.

## 2. Theory

---

More specifically,  $Q$  is calculated for the net air flow in and out of the system as

$$Q = \dot{m} \cdot c_p \cdot \Delta T = \dot{V} \cdot \rho \cdot c_p \cdot (T_2 - T_1) \quad (2.14)$$

Here  $\dot{m}$  is the mass flow rate, computed by volume flow rate  $\dot{V}$  and density  $\rho$ ,  $c_p$  is the specific heat constant for the material and  $\Delta T$  is the temperature difference between inflow and outflow air in this case.

# 3

## Method development

The work process for generating a method for simulating interior climate in buses are described in this chapter. Both the work flow and the chosen best practices are presented.

During the method development, reference works in the industry presented in articles together with previous work within the company are used as a set of first guidelines. Siemens' guidelines for Star CCM+ presented in the user manual documentation and Siemens' method suggestions presented on the online portal *The Steve Portal* are also used as a starting point when developing the method.

The tools used are ANSA for pre-processing and Star CCM+ for meshing, solving, and post-processing. Test results from physical testing will be used for validation of simulation results. From here on name on settings in Star CCM+ are written in italic letters.

### 3.1 Components in the HVAC system

The HVAC system is used to ensure climate comfort and good air quality. There exists regulations and laws for working environment conditions for the driver. The temperature has to be within a certain range to be an acceptable working environment[11]. The climate system behaves differently depending on the outside environment, i.e. the ambient temperature. In cold weather the system is in heating mode, and in hot and humid weather the system needs to cool down the interior air.

The HVAC system consists of 3 main components. The **AC unit**, noted as 1 in Figure 3.1, is located on the roof has the ability to transport heat from inside the bus to the exterior environment with an evaporator when in cooling mode. It is also equipped with a heat pump and can heat the interior air when in heating mode. The heat pump allows more heat energy to be added into the bus than the electricity power input due to extracting heat from the environment. The evaporator allows the bus to be cooled by more than the electricity input, due to extracting heat from inside the bus and releasing it to the environment. This extra efficiency works within a range of ambient temperatures.

**Convectors and heat blowers**, noted as 2 and 3 in Figure 3.1, have the purpose of transporting heat energy from one fluid to another, in this system from a heated water system to the interior air. Heat exchangers enlarge the heated surface area of which the heat can be extracted by the air. Convectors use natural convection to spread the heat while fans have been added to the heat blowers to increase the spreading through forced convection.

The **defroster**, noted as 4 in Figure 3.1, is located in the front and is a combination of a heat exchanger and an evaporator. This keeps the windscreen clean from ice and fog as well as enhancing the driver's climate.

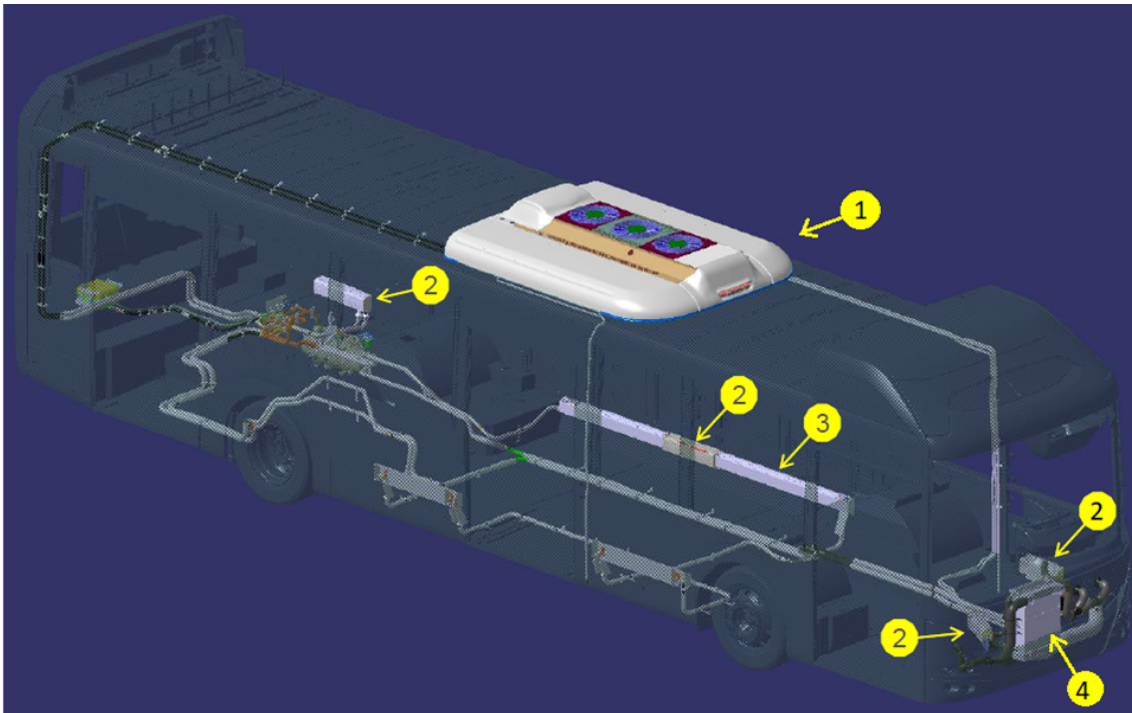


**Figure 3.1:** Location of HVAC components. 1 is the AC unit, 2 and 3 are heat blowers and convectors respectively, and 4 is the defroster unit.

## 3.2 Mesh construction

To construct a suitable mesh the components of interest were imported into ANSA. The bus was divided into three submodels, front, back and mid, and handled that way in ANSA for simplicity. Each submodel of the bus were prepared through highlighting regions of interest that needed special mesh settings due to complicated geometry and regions that would later be assigned to boundary conditions. ANSA was also used to fill small holes and to repair the model where parts were missing or gaps existed. All changes of geometry were made in ANSA to be traceable. After preparation in ANSA the model was imported in Star CCM+ where a mesh was created.

The strategy for meshing was firstly based on guidelines from in-house methods. The goal was to create a closed computational domain of the region of interest, in this case the interior of the bus. Because of this it was of high priority that the geometry details of the bus interior did not change from their original shape due to meshing, see Figure 3.2. The meshing was an iterative and time consuming process but also a very important work to be able to create a mesh of good quality with as few cells as possible. A good mesh strategy is crucial and all following method development is dependent on a good quality mesh. The following sections describe the mesh construction steps in chronological order.

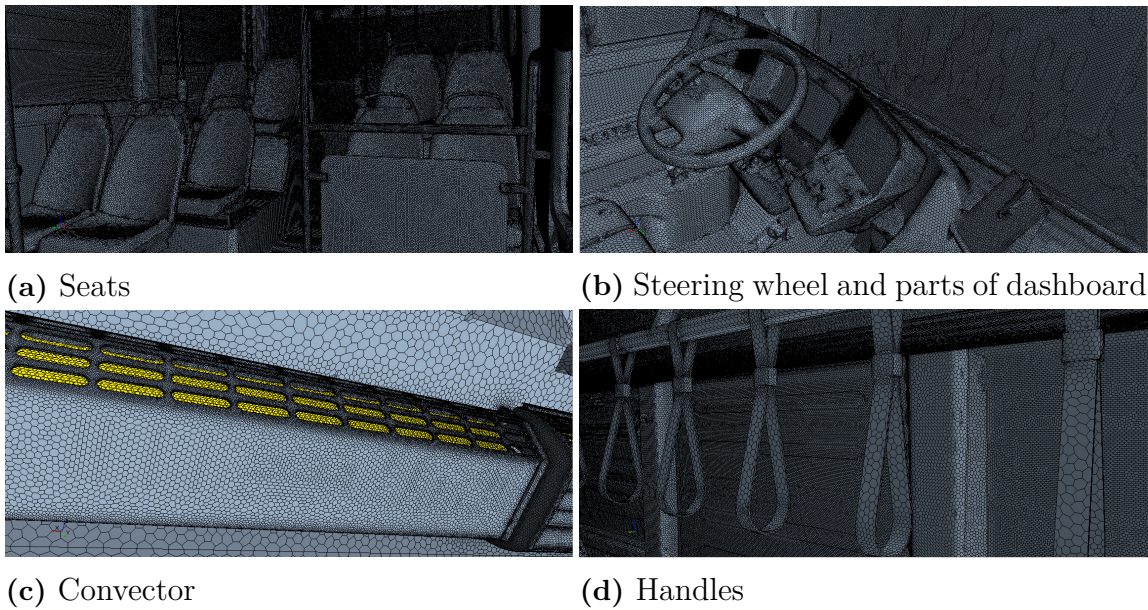


**Figure 3.2:** Details of the meshing.

### 3.2.1 Surface Wrapper

The surface wrapper is a mesh operation in Sar CCM+ commonly used for complex geometries. It performs a closed, non-intersecting surface mesh. A thought through surface wrapper can simplify the volume meshing. Performing a surface mesh in Star CCM+ enables the meshing to be more automated compared to performing this pre-processing in ANSA.

Based on the in-house guidelines one first method was developed to accomplish the mesh strategy. The method was to use an external wrapper and then an internal wrapper to create the computational domain. The external wrapper use the outer shell of the bus and closes the domain with all details kept inside. The internal wrapper wraps the bus from the inside to close small gaps but with finer settings to keep all details. Using this method the simulation diverged. Probably due to spaces created between the external and internal wrappers e.g. pockets inside the bus wall. This led to spaces that was not part of the computational domain and with poor mesh quality i.e. useless for the simulation. An example on one of those problem areas are shown in Figure 3.3.

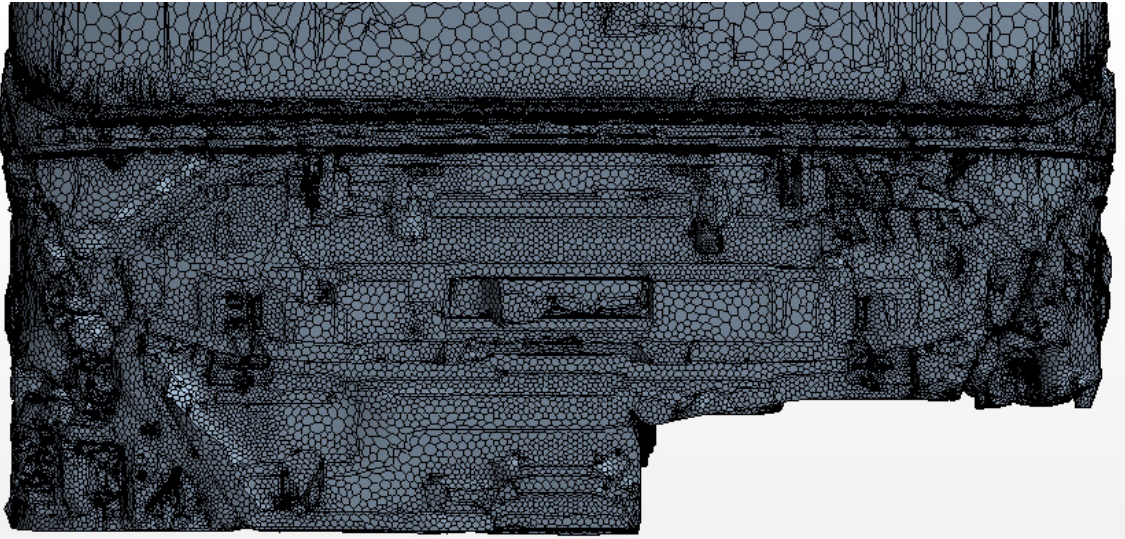


**Figure 3.3:** Mesh with external and internal wrapper, bad example on meshing the lower part of the front.

To avoid getting this problem areas a new method was tried out. The external and internal wrapper was replaced with two internal wraps. One rough wrap that wraps the inside shell of the bus to get a closed computational domain. This rough internal wrapper does not include the pockets created by the external wrapper in the first method. Then the fine wrap will wrap the inside with all details in the interior to make sure that the geometry of the parts will not change. With this method the unnecessary spaces could be avoided, see Figure 3.4. Figure 3.3 and Figure 3.4 shows the same part of the bus with different meshing methods.

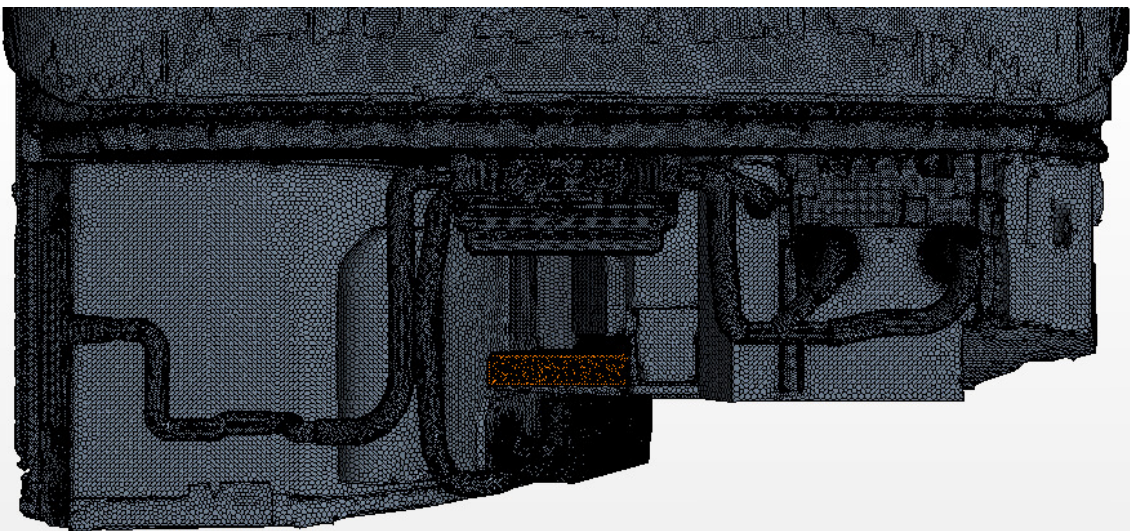


**Figure 3.4:** Mesh with two internal wrappers, good example of meshing the lower part of the front.

A summation of what settings for sizing of the surface cells for the rough and fine internal wraps are presented in Table 3.1 and Table 3.2 respectively.

<b>Default Settings</b>	
<i>Base Size</i>	100 mm
<i>Target Surface Size</i>	100 mm
<i>Minimum Surface Size</i>	35 mm
<i>Gap Closure</i>	35 mm
<i>Proximity Refinement</i>	none

**Table 3.1:** Rough wrapper size settings.

<b>Default Settings</b>		
<i>Base Size</i>	100 mm	
<i>Target Surface Size</i>	20 mm	
<i>Minimum Surface Size</i>	10 mm	
<i>Gap Closure</i>	none	
<i>Proximity Refinement</i>	yes	
<b>Custom Surface Controls</b>		
<b>Parts</b>	<b><i>Target Surface Size</i></b>	<b><i>Minimum Surface Size</i></b>
Air duct	5 mm	2 mm
Bars and handles	10 mm	3 mm
Larger base parts	30 mm	10 mm
Defroster	5 mm	2 mm
Doors	10 mm	5 mm
Heaters	5 mm	1 mm
Ventilation holes	1 mm	0.5 mm

**Table 3.2:** Fine wrapper size settings.

### 3.2.2 Volume mesh generation

With the automated mesh operation a volume mesh can be generated. The automated mesh uses the mesh from the surface wrapper as a starting point for creating a volume mesh. From guidelines polyhedral cells were used in this volume mesh. Thanks to that the wrappers sealed the domain the automated mesh could be created without worrying about new messy areas.

Next step was to ensure that it was possible to get a solution. This means that the mesh has to be of such good quality that the computer will be able to run the simulation without divergence. When this was fulfilled it was possible to investigate  $Y+$  values. High  $Y+$  values can lead to an inaccurate solution due to the wall treatment. Most of the areas with high  $Y+$  values appeared due to large cells. This was solved through decreasing the cell size on the parts surface.

Through the mesh study a lot of different mesh settings were tested in different combinations named 1-4 in Table 3.3. In Table 3.3, number of cells, time for automated meshing and computational time are displayed. For these values the simulations have been run on the same amount of cores.

### 3. Method development

---

The different meshes in the table are going from lowest number of cells to highest i.e. from coarse to fine mesh. The goal was to find a mesh with as few cells as possible due to computational costs but that still could fulfil all the demands.

	Mesh 1	Mesh 2	Mesh 3	Mesh 4
Number of cells	40 000 000	70 000 000	100 000 000	200 000 000
Mesh time	2h 41 min	3h 14 min	3h 42 min	5h 48 min
Computational time for 10 000 iterations	3h 56 min	7h 19 min	12h 8 min	20h 21 min

**Table 3.3:** Results of Mesh Study.

It is also important to get a stable solution that is not fluctuating between iterations. First focus was on keeping all details in the bus and then let the size of the cells increase and grow into the middle of the bus, see Figure 3.5. This resulted in an unstable solution with temperatures that fluctuated. Since the computational domain is the whole interior of the bus and temperatures will be investigated through the whole region the mesh has to be of the same accuracy through the whole domain. An example of this is shown in Figure 3.5.

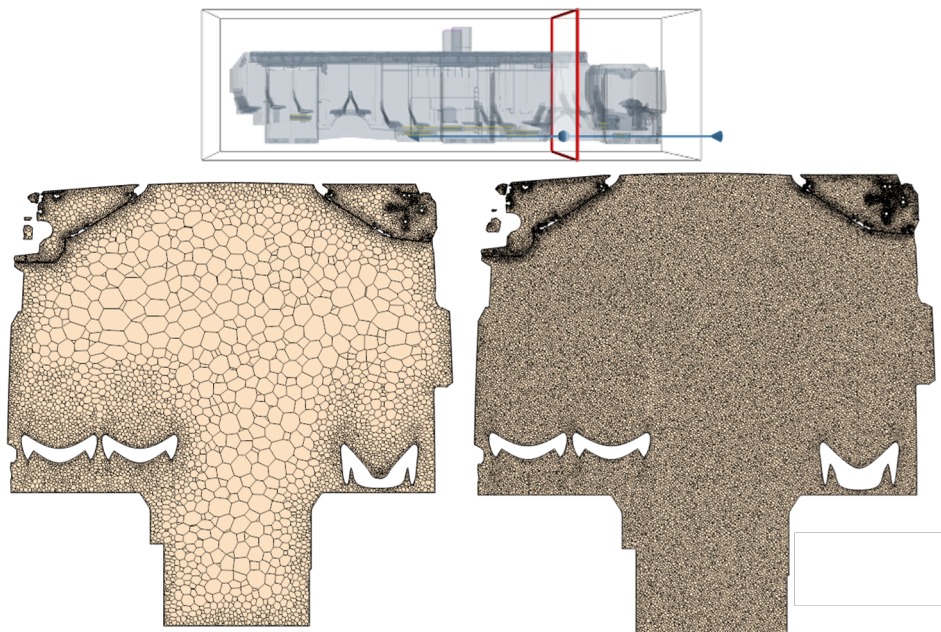
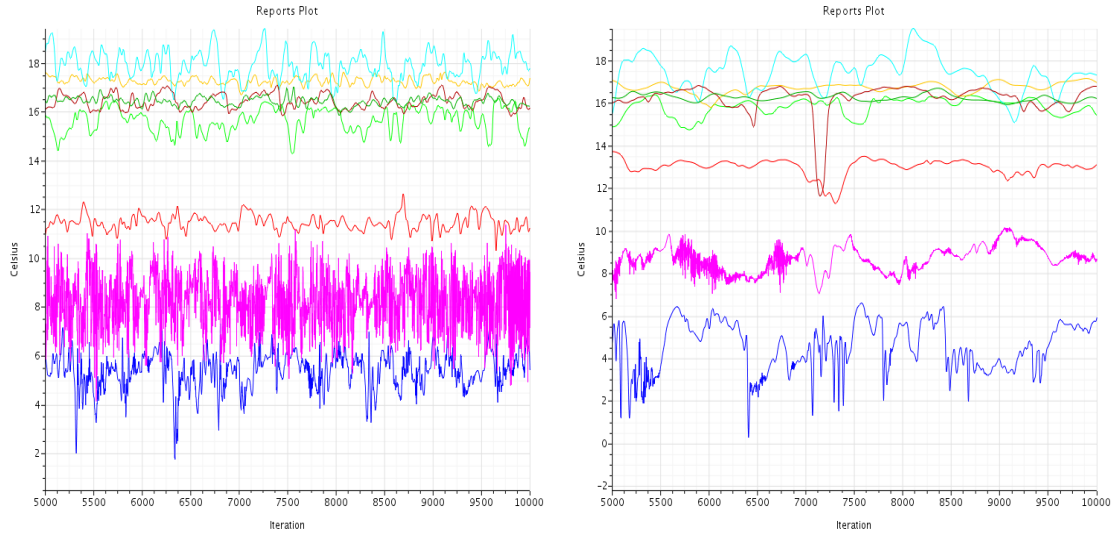


**Figure 3.5:** Example of meshes shown in a cut plane. The mesh to the left have increasing cell size while the one to the right have the same cell size through the whole domain.

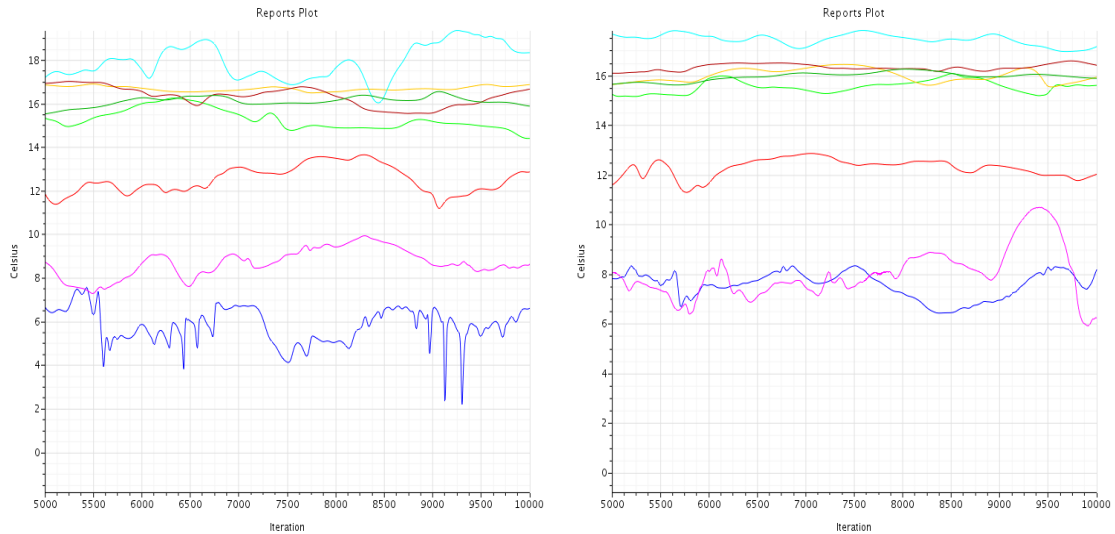
How the increase of number of cells throughout the domain influence the stability of the solution are presented in Figure 3.6. The plots represents the result of the four different meshes presented in Table 3.3. The result of mesh one are shown in plot 3.6a and the result for mesh two are shown in plot 3.6b and so on.

From these results it becomes clear that the stability of the solution improves with an increasing number of cells.



(a) Result of Mesh 1.

(b) Result of Mesh 2.



(c) Result of Mesh 3.

(d) Result of Mesh 4.

**Figure 3.6:** Result of meshes 1-4 in Table 3.3. The temperatures are from measuring points.

The oscillation of the temperature decreases considerably between mesh one and two but also between mesh two and three. The change in stability between mesh three and four are not quite as obvious. Mesh four have about 100 000 000 more cells and a computational time of 20 hours and 21 minutes which is 8 hours and 13 minutes longer than mesh three. The difference in result between these two meshes are small but the difference in number of cells and computational time is large. Due to high computational time and a lack of improved result in mesh four it was decided to work further with mesh number three.

After recommendations, prism layers were added to the mesh on large surfaces that have a large part of the energy transfer to the ambient environment.

The added prism layers will enable to control the  $Y^+$  values on these areas and control how the boundary layer should be resolved. Due to that convection will have a large impact in this method it was beneficial to enable these abilities and to resolve the boundary layer, see section 3.4. The prism layers were added to improve the meshing close to walls, windows, floors and roof since convection at these surfaces are most important.

## 3.3 Simulating physics and solver settings

In this section different physics models and solvers are described together with a motivation of its relevance in the developed simulation method. Some specific modifications from default settings that have been found to be of high importance are presented. The goal was to come as close to default settings as possible when introducing new models, both for simplicity and because default settings can be seen as a recommendation from Siemens.

### 3.3.1 Physics models

In Star CCM+ there are two ways to simulate buoyancy effects due to temperature differences. It can be done either with a constant density solver that adds buoyancy through a source term or by using the ideal gas model that directly solves a varying density. By Star CCM+ user manual the two different models are seen as equivalent. The flow is expected to have a maximum velocity below 100 m/s and below a Mac number of 0.3 in the whole fluid domain, which means that the fluid can be regarded as incompressible due to flow characteristics. Even though the models are seen as equivalent a difference in the flow behaviour can be seen in Figure 3.7. From the figure it is clear that buoyancy is better captured with the ideal gas model. When the ideal gas model is active the temperature rises from the floor to the roof as it is expected to do. This is not the case when the constant density model is active, here the heat is not spreading through the region but stays close to the heat sources. Therefore the *ideal gas* model is chosen for this method and that is also the current best practice from similar simulations.

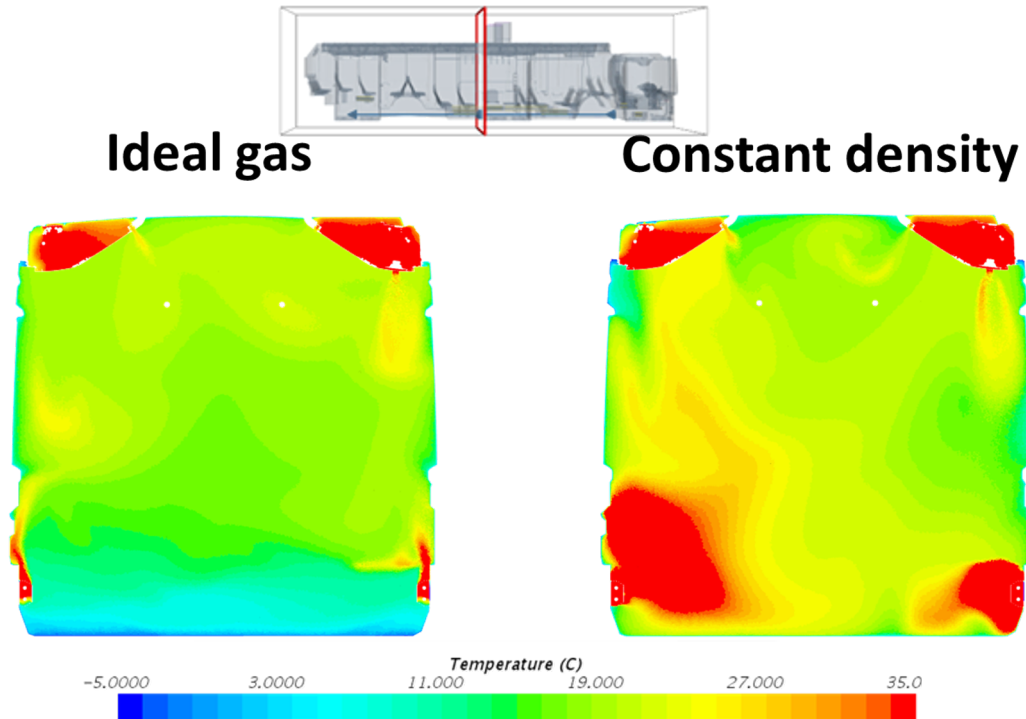


Figure 3.7: Ideal gas and constant density model.

**Gravity** is activated to include the effects the varying density have on the fluid depending on temperature. This induces natural convection in the simulation.

The chosen turbulence model is the  $k-\epsilon$  model because it is a well known, developed and widely used method in the vehicle industry[12]. This model allows a higher  $Y+$  value up to  $\approx 100$  but works best in the range of 30-50. Other turbulence models require  $Y+$  values in the range of  $\approx 1-5$ . The **Two Layer all  $Y+$  Wall Treatment** model is a hybrid between low and high value models. This means that it works good for  $Y+$  values lower than 5 and for  $Y+$  values higher than 30. It also gives reasonable results in the buffer layer i.e. for  $Y+$  values between 5 and 30. If the natural convection is dominant compared to forced convection it is recommended to change the *Two-layer Type* to *Bouyancy Driven (Xu)*[12]. This is an estimation that is valid in regions with low velocity, such as the main volume of the bus domain. Therefore the *Two-Layer Type* is set to *Bouyancy Driven (Xu)* in this model.

**Segregated flow** is a model that solves each of the momentum equations in turn. The linkage between momentum and continuity equation is achieved with a predictor-corrector approach. This model is recommended for mildly compressible flows, i.e. this kind of simulations with low Re numbers and no need of shock-capturing. Advantages with the segregated solver is a lower demand of computational resources and easier convergence. It is also recommended from in house guidelines.

### 3. Method development

---

The in Star CCM+ chosen physics models for this method are presented in Table 3.4. Some of the models are recommended by Star CCM+ and therefore selected automatically. Some of the optional models are chosen based on best practice guidelines at the company but have not been studied.

<b>Group box</b>	<b>Model</b>
<i>Space</i>	<b>Three Dimensional</b>
<i>Time</i>	<b>Steady</b>
<i>Material</i>	<b>Gas</b>
<i>Flow</i>	<b>Segregated Flow Gradients</b> (Selected automatically)
<i>Equation of state</i>	<b>Ideal Gas</b>
<i>Energy</i>	<b>Segregated Fluid Temperature</b>
<i>Viscous regime</i>	<b>Turbulent Reynolds Averaged Navier Stokes</b> (Selected automatically)
<i>Reynolds-Averaged Turbulence</i>	<b>k-<math>\epsilon</math> Turbulence Exact Wall Distance</b> (Selected automatically) <b>Realizable k-<math>\epsilon</math> Two-Layer</b> (Selected automatically) <b>Two Layer all Y+ Wall Treatment</b> (Selected automatically)
<i>Optional models</i>	<b>Gravity</b> <b>Cell Quality Remediation</b> <b>Proximity Interpolation</b>

**Table 3.4:** Physics Models

**Radiation** is costly to simulate but is of high importance in cases of objects with high surface temperatures and needed in cases with solar loads. A study has been performed with simulations with and without the radiation active and the results have been compared to evaluate if radiation has a large impact on the simulation results. If the difference from activating radiation is small, or the total accuracy of the results are not affected, the model option can be left deactivated as it can be assumed to be negligible. Solar loads are not included in the method due to how experimental tests were performed, see section 3.5.1.

With radiation a couple of more physics models are added:

<b>Group box</b>	<b>Model</b>
<i>Optional Models</i>	<b>Radiation</b>
<i>Radiation</i>	<b>Surface-to-Surface View Factors Calculator</b> (Selected automatically)
<i>Radiation Spectrum</i>	<b>Grey Thermal Radiation</b>

**Table 3.5:** Radiation Physics model settings.

As mentioned, radiation extends the computational time. In this model it has been found it took three times longer to run a solution with radiation compared to a simulation without radiation. Due to this it was decided to investigate how much impact radiation has on the result. After this a decision about if radiation is worth its time can be taken. This is why the physic models for radiation is not included in the first set up of physics models.

### 3.3.2 Solver settings

*Under-relaxation factors* are modified to reach stability in the solution convergence. A lower value typically means a more robust and stable simulation but requires more iterations until it is fully converged. It has been found that the under-relaxation factors in segregated flow for pressure and velocity needs to be lower than default. To avoid divergence in the beginning of the simulation when implementing a pressure specified inlet boundary, see section 3.4, the under-relaxation factors have to be linearly ramped. Except these changes the solver settings are set to default.

## 3.4 Boundary Conditions

In Star CCM+ the boundary conditions were modelled in different ways to be as close to reality as possible. The boundary conditions consist of the HVAC system described in section 3.1 and the walls of the bus. This section describes how each type of boundary condition has been modelled together with an explanation of what effects this method have on the simulated physics.

**Inlets:** The AC is modelled as a black box and replaced with two air inlets on the roof, see Figure 3.10. One inlet is connected with the left air duct and the other one to the right air duct. The pressure is controlled at these inlets by assigning them to pressure *Stagnation Inlet*. The pressure is calibrated until the total volume flow matches a volume flow specified by the manufacturer of the fans. In this case the left air duct have smaller holes where the air can enter the bus and thus more resistance for the fans. Due to this the air flow will be less in this air duct. The right air duct has larger holes, especially where the doors are mounted. This side will therefore have less resistance and thus more air flow which can be seen in Figure 3.8.

### 3. Method development

---

By assigning the inlets to pressure inlets the difference in resistance will be taken into consideration and the pressure distribution will be equal in the both ducts.

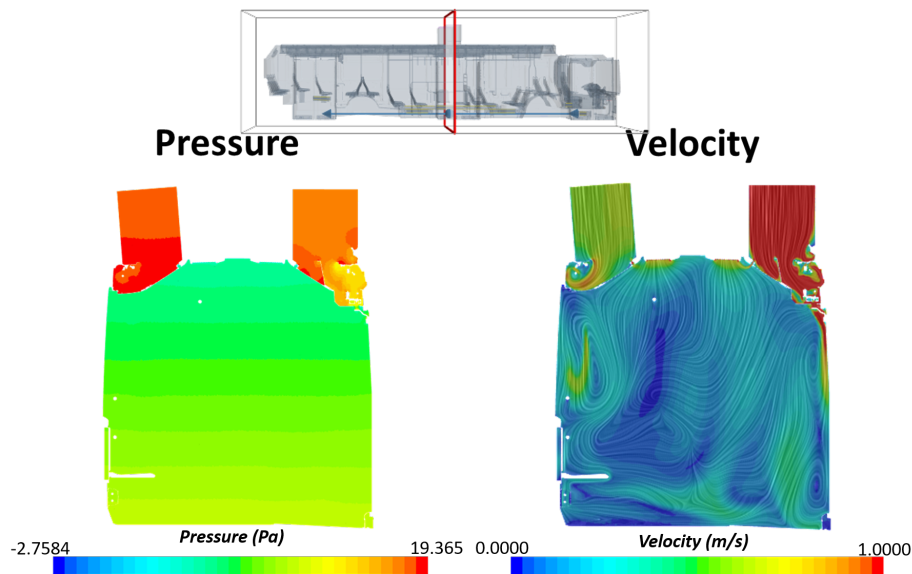


**Figure 3.8:** Both pictures above are assigned to stagnation pressure inlets. The left figure shows the pressure distribution in the air ducts while the right figure shows the velocity distribution.

Another tested option was to specify the inlet for the AC to a velocity inlet where the velocity is computed so it matches a total volume flow. This means that the air flow will be equal in the two air ducts, see Figure 3.9. This led to pressure differences in each air duct due to the difference in resistance, see Figure 3.9. The fans are not controlled this way and this method did not catch the real behaviour of the fans in the bus.

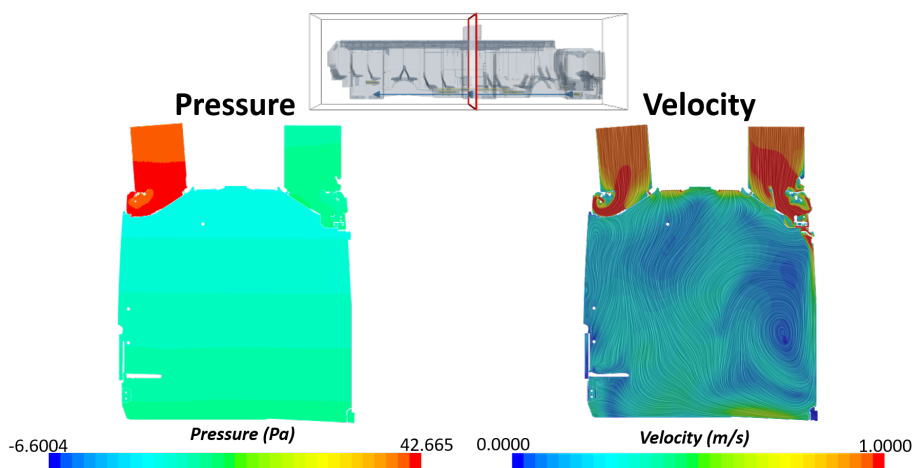


**Figure 3.9:** Both pictures above are assigned to velocity inlets. The left figure shows the pressure distribution in the air ducts while the right figure shows the velocity distribution.

The defroster inlet, see Figure 3.10, is set as a velocity inlet where the velocity is computed so it matches a total volume flow. This volume flow comes from manufacturer data. The inlet can be defined as a velocity because it is only one surface i.e. same resistance for all air flow compared to the the AC-unit that has two inlets.

As a summary the inlet for the AC is set with a pressure while the defroster inlet is set with a velocity. Both inlets have a specified temperature. The temperatures are set to experimental values.

**Outlets:** When choosing outlet boundary types it is important that the total mass flow into the bus matches what is flowing out of the bus. Secondary, it is good to control how much mass is flowing through each outlet to verify that the simulation resembles a system that uses 100 percent re-circulation air for the defroster and AC respectively. This means that what mass flows in from the defroster inlet should leave through the defroster outlet and the mass flowing in from the AC inlet should leave through the AC outlet. Setting the outlet to a *Pressure Outlet* of 0 Pa compared with a reference pressure of atmospheric lets the entering air to flow out of the bus. The temperatures are specified at these outlets as experimental values measured at locations close to the outlets. The outlets both for the defroster and the AC-unit are marked in Figure 3.10.

Star CCM+ has a function to calibrate the outlet pressure until the mass flow matches a specified value. However this pressure calibration would change the mass flow entering the bus since the AC inlet boundary is defined with a pressure difference compared with a reference pressure of atmospheric. Therefore, the outlets are left as pressure outlets with 0 Pa. The total mass flow over each outlet can be monitored and observed to not deviate too much from the inlet mass flows. This boundary definition can be further studied for a finer calibration.

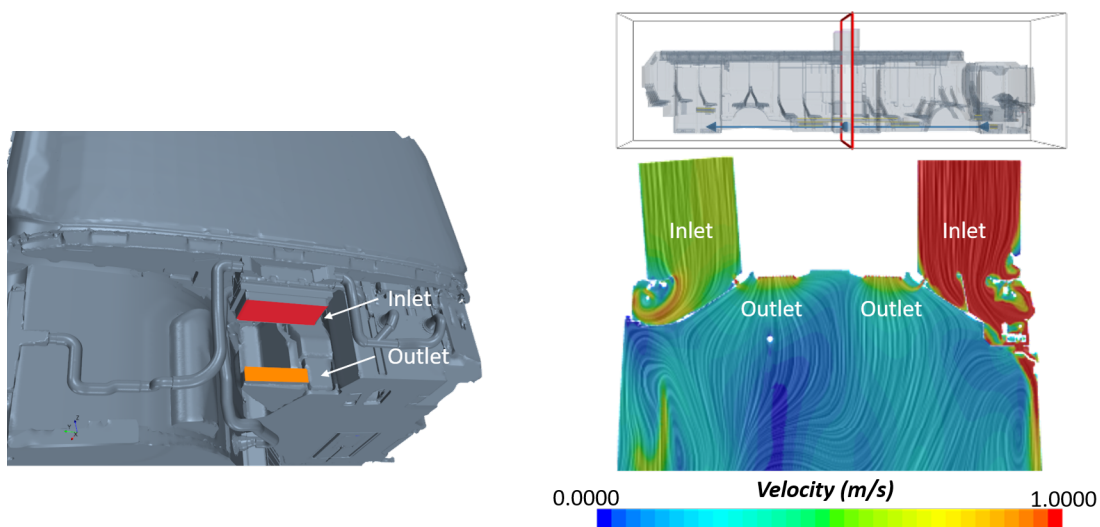


**Figure 3.10:** Inlet and outlets for the defroster, to the left, and AC-unit, to the right.

**Convectors:** The convectors can be modelled with choosing the setting called *Energy Source Option* to the option *Heat Exchanger* in Star CCM+. This option can then be modified in multiple ways. The most stable way has been found to be by creating separate regions for each heat exchanger and having interfaces between the heat exchanger regions and the main fluid domain. These interfaces are located at the inlets and outlets of the heat exchangers. Having a separate region means that the heated element is wrapped and meshed in a separate operation, and that the interface surfaces have to be marked beforehand in ANSA to be able to select and mark interfaces in Star CCM+. The convectors have a total energy rate that depends on its length multiplied by a heat rate per meter that is set to be constant for each simulation. This means that a longer convector can give off more heat energy than a shorter convector. The heat rate per meter depends on the temperature difference between the heated water of the heat exchanger and the air in the bus. In Figure 3.11 a cut plane of the convectors and how the heat is spreading from them is shown.

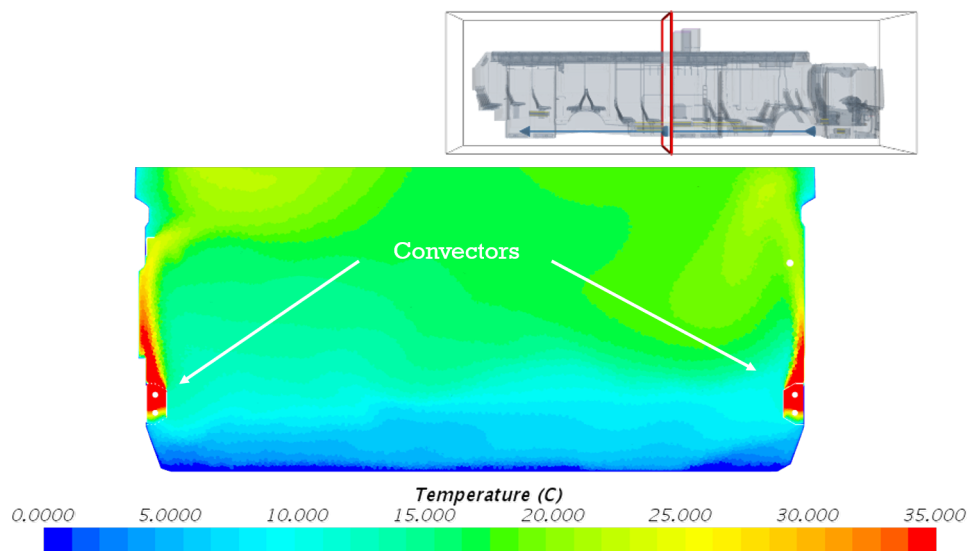


**Figure 3.11:** Convectors in the middle of the bus.

**Heat blowers:** The heat blowers are modelled as the convectors but with a constant total energy rate, even if the lengths of the component vary. In Star CCM+ the *Momentum Source Option* is chosen to the option *Specified* to simulate the fans and the value is entered to match manufacturer data of volume flow through the heat blowers. The *Upstream Interface Boundary* is the bottom surface where cold air enters the exchanger, the *Downstream Interface Boundary* is the top surface where heated air leaves the exchanger. Heat blowers are only activated when doors are open and the bus temperature is below the set temperature. When the heat blower is not activated it works in the same way as a convector.

**Convection:** To simulate the heat leaking out from or into the bus a heat transfer coefficient is put to the exterior parts of the bus chassis. This will let heat being transported through the walls, roof, floor, windows and doors of the bus. In this model, losses from air leaking through small gaps are not taken into consideration separately. Instead a simplification is made, all different reasons for leakage of heat energy are included in this heat transfer coefficient hereafter abbreviated as HTC. Another simplification is to put a single HTC for the whole domain. The HTC will be used as a calibration constant and this simplification keeps down the number of calibration settings to investigate. This can result in a total temperature in the bus being calibrated well but temperatures in specific regions might deviate from experimental values. To get results closer to reality the HTC should vary in different regions of the bus. This simplified method will also result in a higher value on the calibrated HTC than in reality due to that all leakages in the bus are included in this coefficient. This boundary condition value is unknown and was swept, see section 3.5.2.

## 3.5 Model calibration with experimental data

After the method settings were investigated and chosen the set of unknown physics constants could be calibrated on the chosen mesh. A sweep of different HTC values were conducted to find the setting that best correlate to known experimental data.

### 3.5.1 Collection of experimental data

The experimental data was extracted from testing done in a climate chamber. The experimental data was taken from the end of pull-up and pull-down tests. These test represents the heating or cooling of the bus in the beginning of a shift. First the bus is turned off in ambient temperature long enough for the interior of the bus and all components to reach the ambient temperature. Then the bus was cooled or heated to set temperature. When the sensors had stabilised and the bus was determined to have reached a steady state the temperatures could be extracted. The doors were closed and 100 % of the air going through the defroster and AC unit were taken from re-circulation. This means that all added heat energy is lost by convection or leakage through the exterior of the bus and the bus is in a steady state.

Since the used experimental data was measured in a chamber with no solar loads, this also motivates the limitation of not applying solar loads in the simulations. Temperatures were measured at eight locations in the bus in the experiment. The first six points were placed at two different heights in the middle of the walkway at the front, middle and back of the bus, see Figure 3.12. The last two points were used to compute a set temperature in the bus which the HVAC system is controlled by. These two points were located below a seat in the back left of the bus and in the top of the bus close to the re-circulation air intake of the AC unit. These two controlling temperatures are weighted respectively and summed to compute the set temperature in the bus. The locations and weighted summation of these points are aimed to reflect the average temperature of the bus.

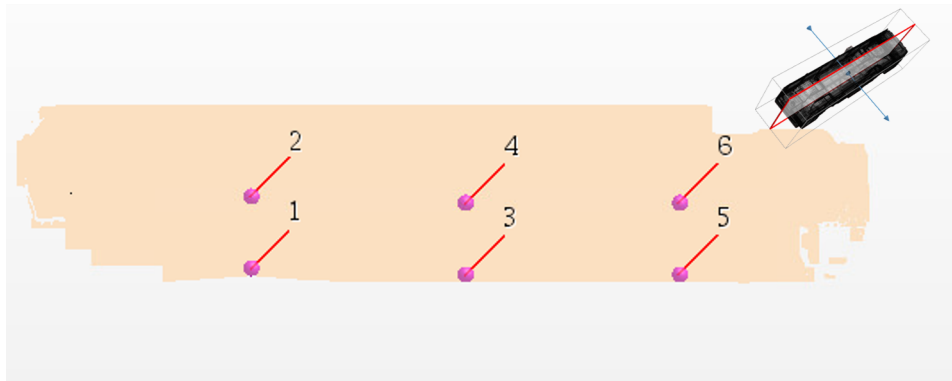


**Figure 3.12:** Position of points where the experimental data is measured.

The collected data are from two different cases. One warm case with ambient temperature of 32 °C and one cold case with ambient temperature of -4.5 °C.

#### 3.5.2 HTC sweep

A converged solution is needed to calibrate the model with experimental data from a steady state case. If the solution is oscillating around a constant mean value an averaged solution can be used. If a more irregular oscillation is occurring, the sample frequency of the averaging can be controlled. By doing this irregularities of certain frequencies can be excluded. This is done to get a valid converged temperature to calibrate with. The *Field Mean* option can be used in Star CCM+ to accomplish this and has been found helpful in this model development.

After all known boundary conditions were implemented the convection parameter needed to be swept. Different HTC values give different temperatures in the simulations. For the cold case a larger HTC gives a cooler bus because more heat is leaking out through the exterior panels. For the warm case a larger HTC gives a warmer bus because more heat is coming into the bus from the outside environment. The idea was to simulate a range of HTC values and capture a HTC value that would make the temperature in a point match the experimental value. The first value of the sweep was set after guidelines on other vehicle simulations together with an estimation of how much total heat flux is leaving the bus through a known area.

### 3.6 Summation of method development findings

This section is a summary of the generated method with highlights on important findings.

A mesh strategy was time consuming to develop a robust method for and an iterative process. It is a sensitive part of the development since all further studies are dependent on a detailed mesh with cell qualities that allow for a solution to converge. Specific settings for a mesh construction can vary based on which bus type are to be simulated and what geometry models are available.

The main points of focus for the mesh strategy were the following:

- Create a closed domain that does not include squeezed areas outside of the region of interest.
- Focus on keeping the details of interest, while closing very small gaps and openings that are of no interest.
- Including prism layers in the volume mesh has been seen to help capture convection in a more stable way and also helped to control the  $Y+$  value in regions of higher flow speeds.
- Keeping the cell size down through the whole volume mesh is important since details of the flow and temperatures are of interest through the whole interior of the bus.

The most important findings for solver settings and used physics models are the following:

- Using the  $k - \varepsilon$  turbulence model with the *Two-Layer all  $Y+$  Wall Treatment* is a good choice since the range of  $Y+$  is large through the mesh.
- Ideal gas is found to be the best option to simulate density variation.
- Gravity and a buoyancy driven convection is important to capture the dominant natural convection in a bus.
- Slightly lowering the under-relaxation factors and ramping them in the beginning for velocity and pressure is crucial for a more stable solution.
- Segregated flow solvers are used to keep the computational costs down and keep down required memory.
- Radiation is a computationally costly model to include.

The most important findings for boundary conditions are the following:

- The AC and defroster have been modelled as black boxes. Conditions of the air leaving these units have been measured in experiment and these conditions have been used as boundary conditions. This led to a correct total effect entering the system but made it harder to compute certain event of conditions in-between experimental data reference points.
- Inlets from the AC have been put to a matching pressure to divide the volume flow between the air ducts. The inlet for the defroster has been put to a specified velocity to match a known volume flow.
- Outlets have been put to pressure outlets with a 0 Pa pressure compared with an atmospheric pressure reference.
- Convector and heat blowers have been modelled in separate small regions where a heat energy and momentum have been added to the flow. A pressure drop through the heat exchangers has not been considered specifically but the total volume flow has matched manufacturer data.
- The exterior walls, floor, windows, roof and doors have been put with a single heat transfer coefficient so a total energy rate can leave the bus for an average temperature measurement can match experimental data. This has then been a crucial calibration constant.



# 4

## Results and discussion

In this chapter results from the work is presented together with the result from the HTC sweep.

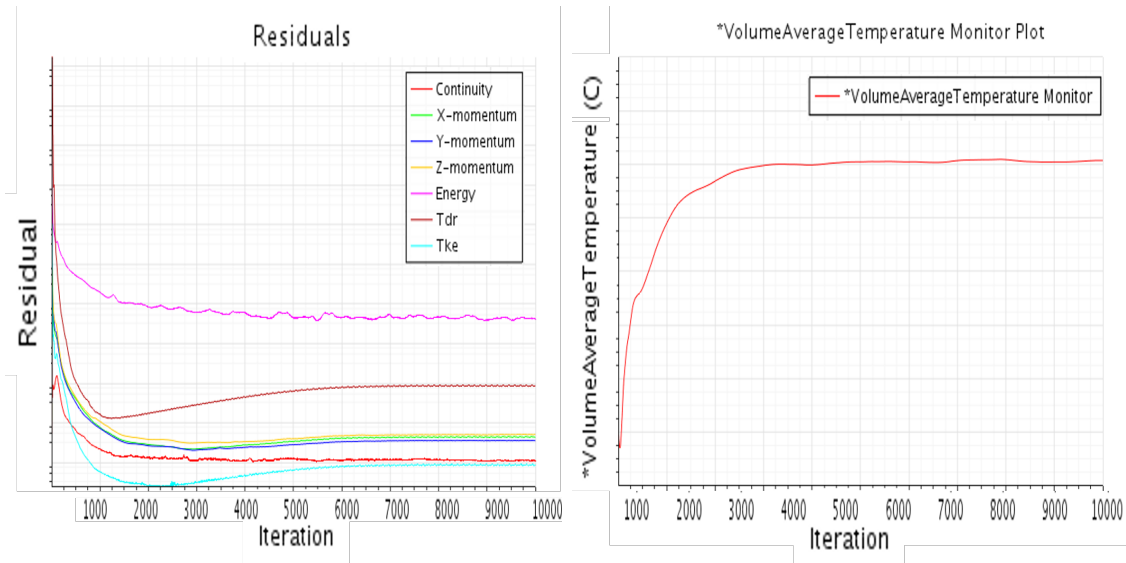
### 4.1 Physics Simulation

This section is dedicated to showing in general how the model is capturing the flow attributes. First the convergence of the simulation is shown. Then the resulting  $Y+$  values for a worst case scenario with maximum fan speeds are shown to validate the mesh strategy and usage of the chosen turbulence model. After that flow shapes are illustrated to show that the model is capturing the expected flow from all components when they are active and following the geometry of the bus in a realistic way. Then the temperature field is presented in three dimensional scenes of the bus and in cut planes. This is followed by showing how the convection through the exterior is captured and in what region there is a higher convection rate.

#### 4.1.1 Convergence

In Figure 4.1 the residuals from the simulation together with the volume average temperature are shown. The residuals have stabilized and are not fluctuating. The same for the volume average temperature, it is stable around a value. This suggests that the solution has converged. In Figure 4.2 the distribution of  $Y+$  values for a worst case scenario, the air flow through the bus is set to maximum, are shown. In this plot it is shown that the  $Y+$  values are in the range where the turbulence model works. This suggests that the mesh is good enough for the simulation to work.

## 4. Results and discussion



(a) Residuals

(b) Volume Average Temperature

**Figure 4.1:** Since there is almost no fluctuations in these plots it can be decided that the solution has converged.

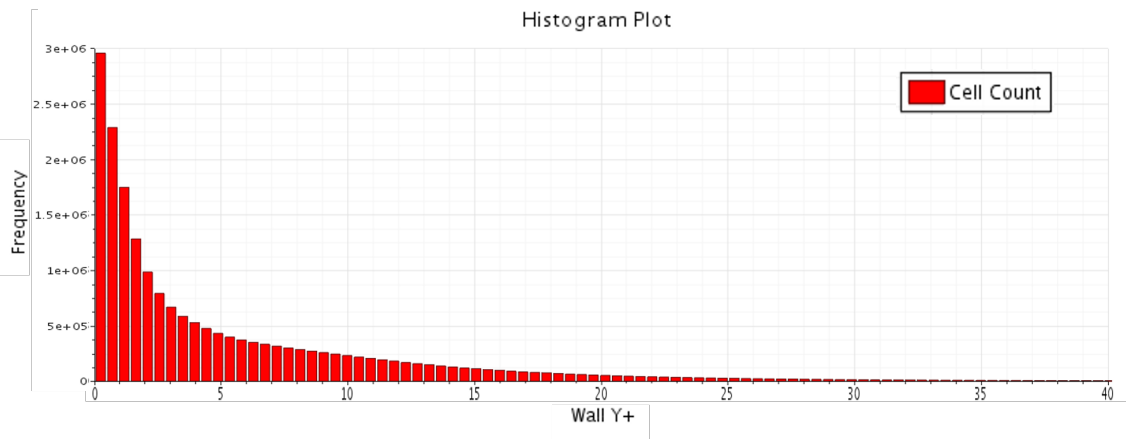


**Figure 4.2:** Histogram plot over  $Y^+$  values for the worst case scenario i.e. when it is maximum air flow in the bus.

### 4.1.2 Flow shape

The flow shape around the geometry details are illustrated in Figure 4.3 - 4.5. It can be seen that the flow is following the details and inlet holes for the defroster in Figure 4.3 and the flow is following the ventilation inlet holes from the air duct in Figure 4.4. This suggests a valid mesh method that have captured the small detailed geometries. The velocity scales in Figure 4.3 and 4.4 are the same with a cap on low speed, these two figures have the purpose of visualizing the flow and not used to analyze velocities numerically. In Figure 4.3 there are high velocities in the pipes coming from the defroster. A lower speed can be noted in the pipe leading to the inlet close to the driver's right knee. This could be because of the momentum of the flow. The momentum makes the flow continue straight forward in the pipe leading to the next outlet at the driver's left knee instead.

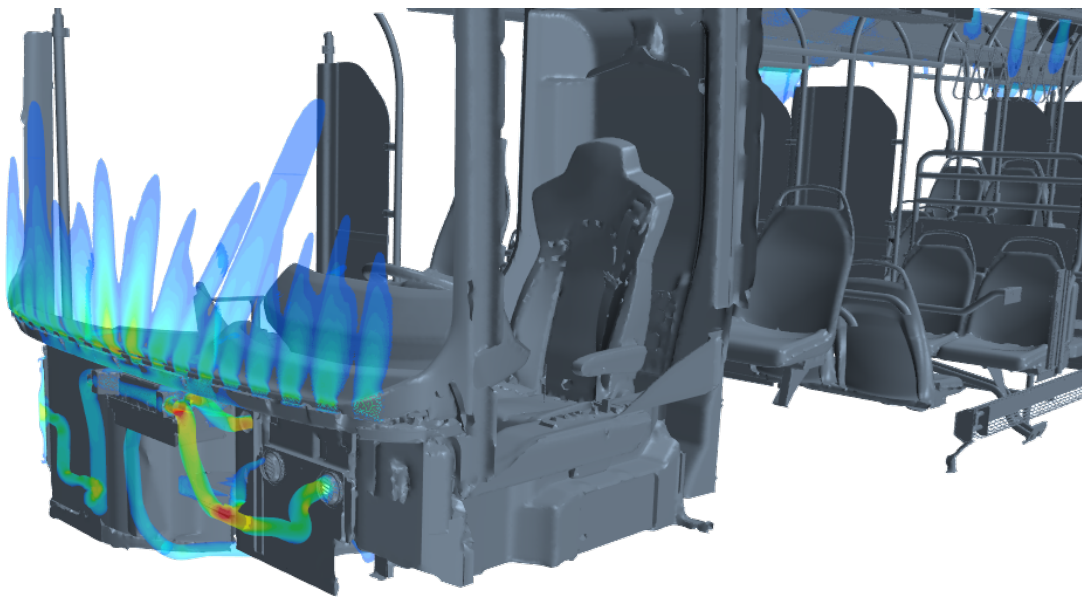


**Figure 4.3:** Air inflow around windscreen, air coming from the defroster. Colouring of the stream represent velocity magnitude, with a cap on low speed.



**Figure 4.4:** Air inflow around left air duct. Colouring of the stream represent velocity magnitude, with a cap on low speed.

In Figure 4.5 it can be seen that a lot of the flow leaving the right air duct is leaving the duct around the doors. This is because there are large holes for the opening mechanism where the air can also flow through. This verifies that more flow is going in the right air duct because of less resistance in that duct.

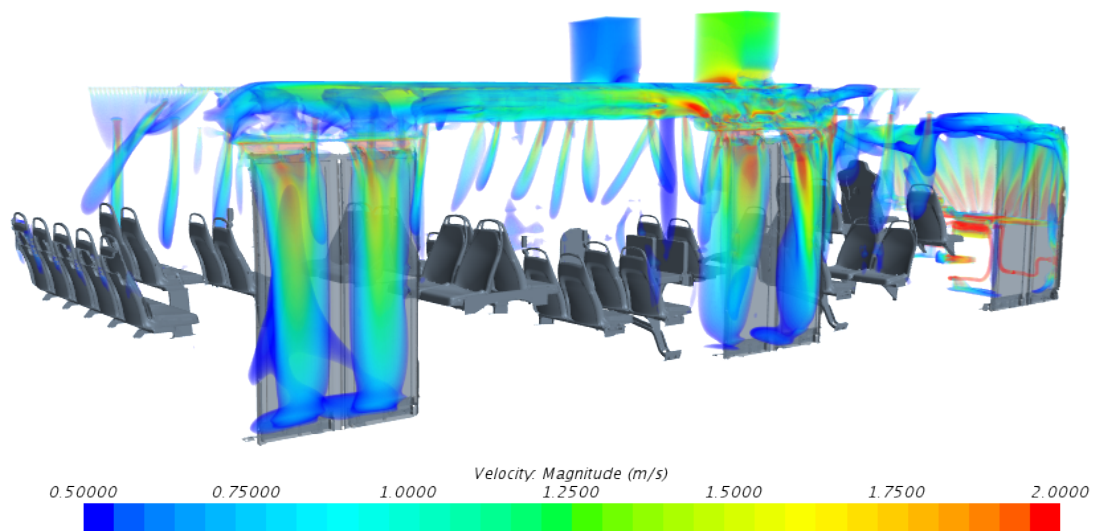


**Figure 4.5:** Air flow shape in the whole bus. Colouring of the stream represent streams of high velocity, low cap on velocity magnitude is 0.5 m/s.

### 4.1.3 Temperature fields

In Figure 4.6 the volume render of cold air in the bus is shown. From this figure it is clear that the bus is cold close to the floor, especially in the middle of the bus.

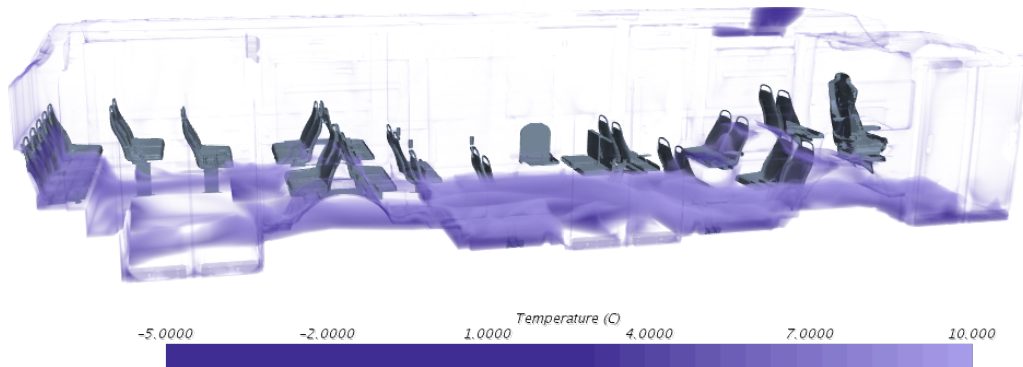


**Figure 4.6:** Volume render of cold air in the bus. Ambient temperature is  $-4.5\text{ }^{\circ}\text{C}$ .

In Figure 4.7 the temperature flow in the right part of the bus is presented. It can be seen how the flow enter the bus through the holes directed at the passengers. Some of the flow from the larger holes at the middle door are also captured.

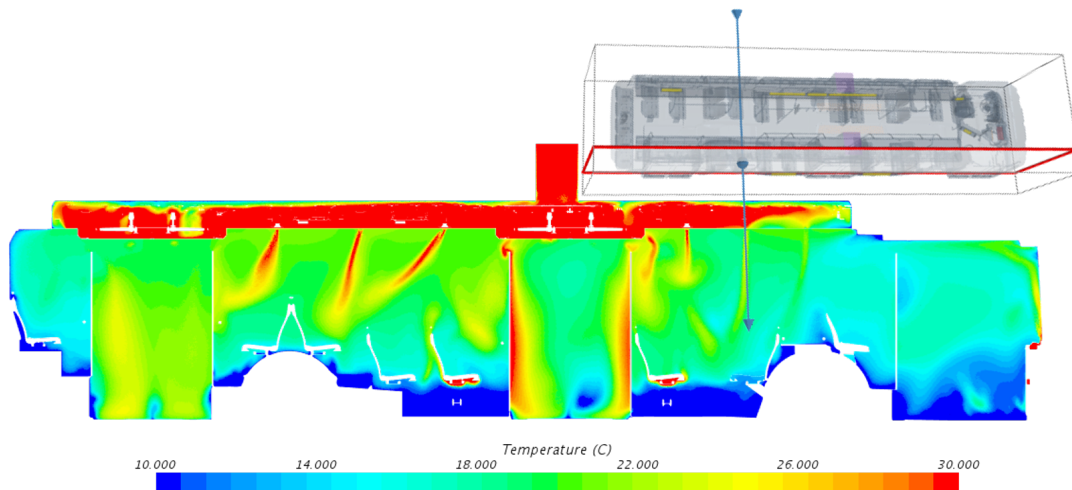


**Figure 4.7:** Temperature flow in the right part of the bus. It can be seen how the flow enter the bus from the air duct.

### 4.1.4 Boundary heat flux

In Figure 4.8 it is shown which parts in the bus have been put to adiabatic in orange and in which parts a boundary heat flux is simulated at by adding convection, in grey.

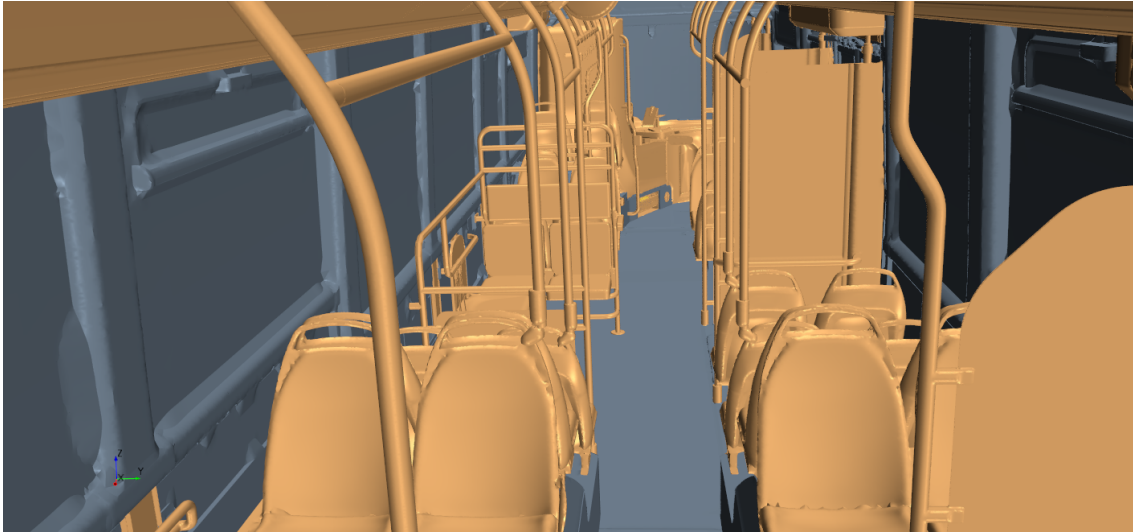


**Figure 4.8:** Illustration of boundary types in the bus.

Figure 4.9 and 4.10 are showing the boundary heat flux on the bus' exterior for the warm case.

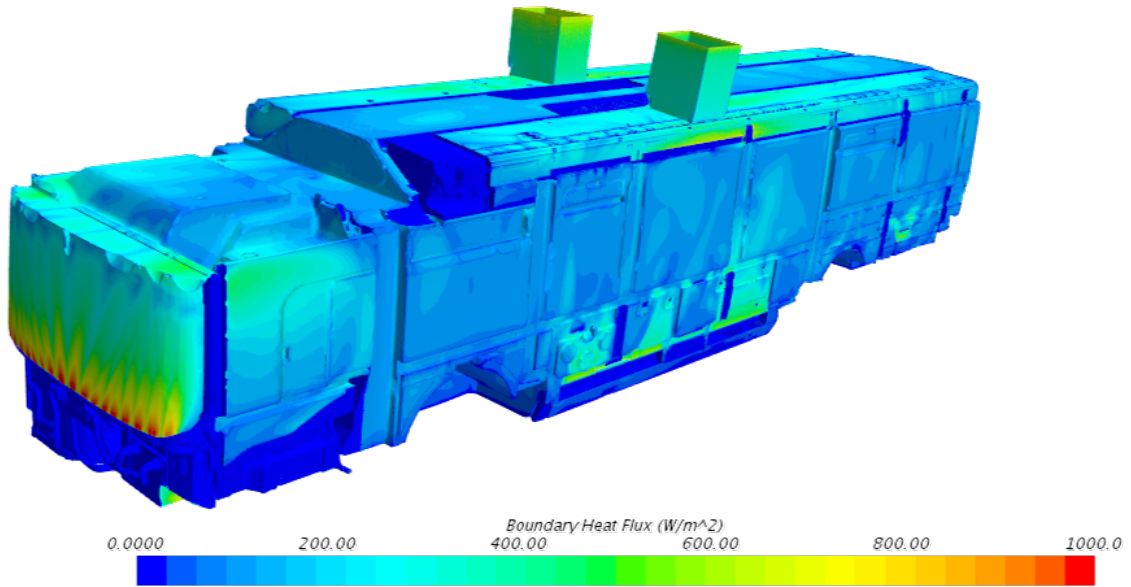


**Figure 4.9:** Boundary heat flux at the front and left wall of the bus.

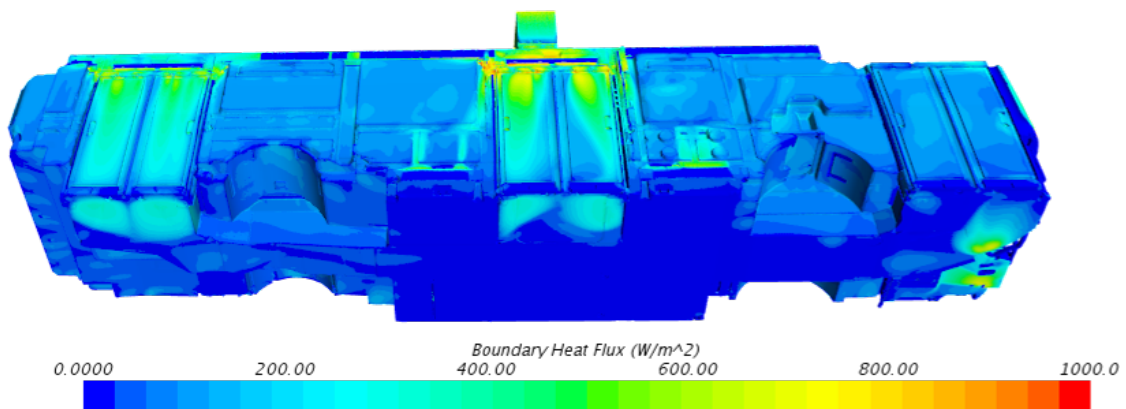


**Figure 4.10:** Boundary heat flux at the bottom side and right wall side of the bus.

In Figure 4.9 it can be seen that a lot of the heat flux is located at the windscreen. This is because warm air is blowing out from the defroster and is a wanted attribute for de-icing of the windscreen. Heat flux is also happening at the walls centered around where heated air is coming from the convectors. In Figure 4.10 it can be seen that a lot of convection is happening around the doors. This is because of the warm air coming from the right air duct. In the middle of the bus there are less convection at the floor. This is because the cold air is gathered there and the temperature difference between interior and exterior is smaller here, which was seen in Figure 4.6.

## 4.2 HTC calibration sweep

The HTC calibration was done on two cases with different ambient temperatures, from now on called: warm case and cold case. Both cases were simulated with and without radiation active. The resulting delta temperatures are shown in graphs below. The graphs present how far from experimental values the simulations are in the different points in the model, measured in °C. The experimental reference value for each measurement point is the bold marked x-axis, the experimental reference value varies between the points. A negative delta temperature means that the simulation is colder than experimental data in the specific point. A positive delta temperature means that the simulation is warmer than experimental data in the specific point. The sweep is done to find the HTC that matches experimental data best i.e. when the delta temperature intersects the x-axis. All values for the HTC have been normalized in the following graphs.

### 4.2.1 Warm case

Results for the HTC sweep of the warm case are presented in this section followed by a discussion of the result's findings. In Figure 4.11-4.13 the temperatures and how they change depending on the value of the HTC is shown. The temperatures are measured at the same positions in the bus as the experimental data. The ambient temperature for the warm case was 32 °C.

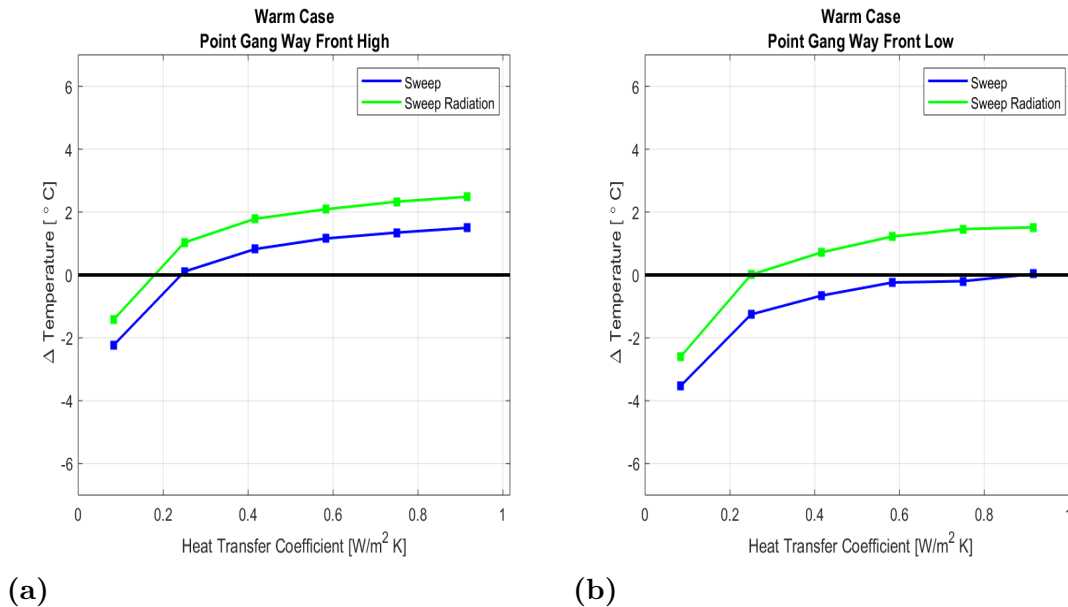


**Figure 4.11:** Warm HTC sweep delta temperatures for points Gang Way Front High and Low.

## 4. Results and discussion

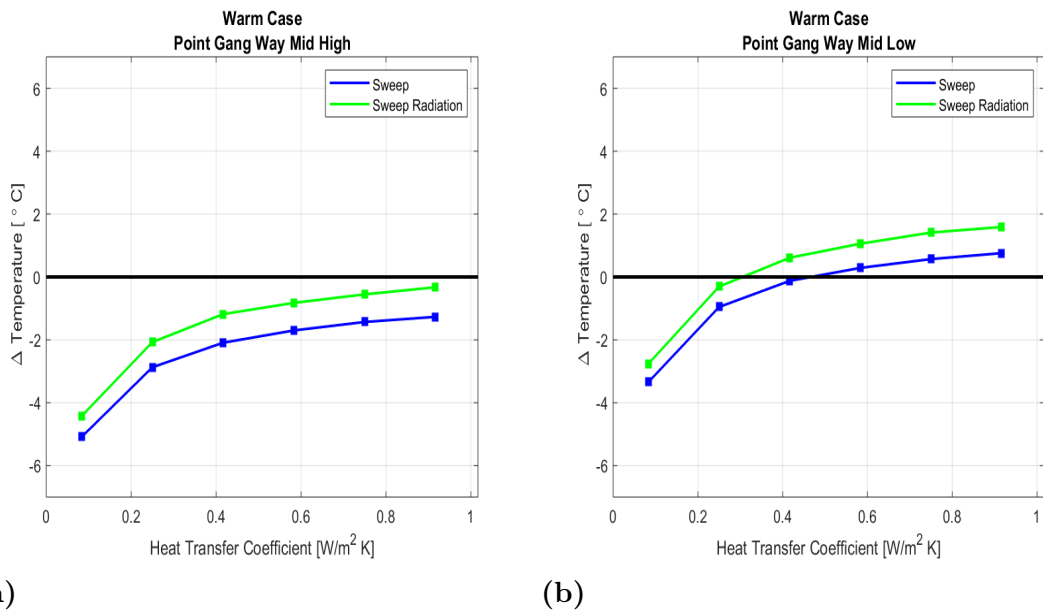


**Figure 4.12:** Warm HTC sweep delta temperatures for points Gang Way Mid High and Low.

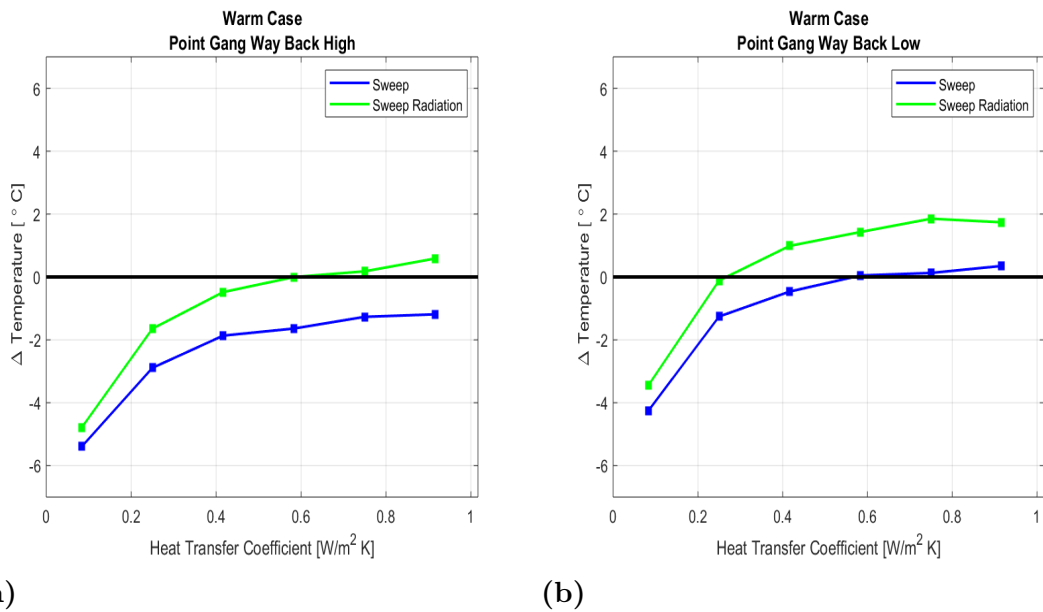


**Figure 4.13:** Warm HTC sweep delta temperatures for points Gang Way Back High and Low.

It can be seen in all graphs above that a higher HTC gives a warmer interior. This goes in line with what was described in section 3.5.2 and shows that more convection is captured with higher HTC values.

The graphs have a steeper slope for lower HTC values. This can be of two reasons. Comparing a low HTC value of for example 0.1 with a higher value of 0.3 is tripling the potential convection effect if the temperature differences through the walls stay the same. Tripling the value again would mean comparing an HTC of 0.3 with an HTC of 0.9. This causes a declining slope in a plot with linear axes. The other cause of the declining slope is that for higher convection the temperatures at the walls get closer to the environment temperature and thus lowering the potential convection effect.

The shape is very similar for all the curves both with and without radiation. In these measured points there is a constant difference in temperature between having radiation active or not. This can mean that more convection is captured with radiation active but it does not affect the temperature spread in the bus.

In Figure 4.14 the average delta temperature, deviation temperature from experimental data, of all six points presented above is computed. By doing this a best HTC value can be chosen, the green and blue round dots in Figure 4.14. All six points have been weighted equally here.

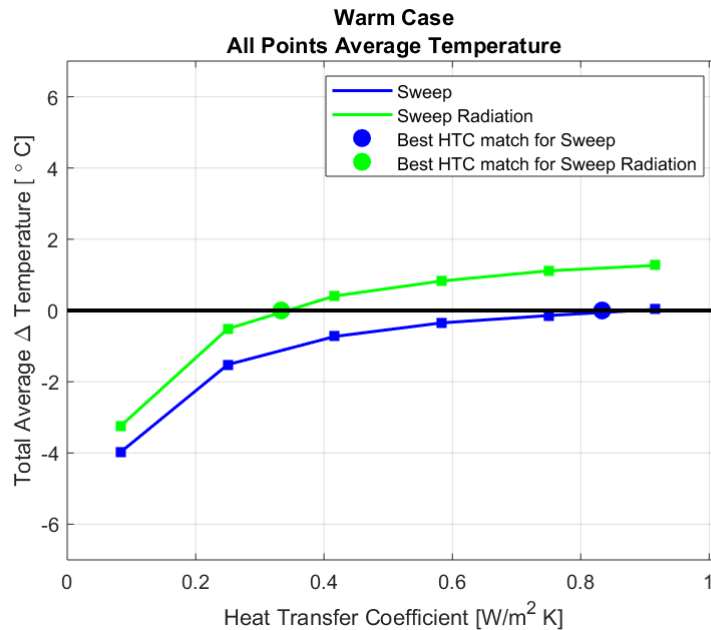


**Figure 4.14:** Average of warm HTC sweep delta temperatures for all points.

By looking at Figure 4.14 the HTC value that gives a best fit with and without radiation can be chosen. It shows that radiation gives a large impact on the HTC value even if there is not a significant improvement for the individual points. By simply looking at these graphs there would not be an improvement by including radiation. However the lower HTC value better match the expectations from guidelines and better resembles a reasonable real value. Including radiation should better capture the real physics, it could also perform differently in areas not analysed closely here.

## 4. Results and discussion

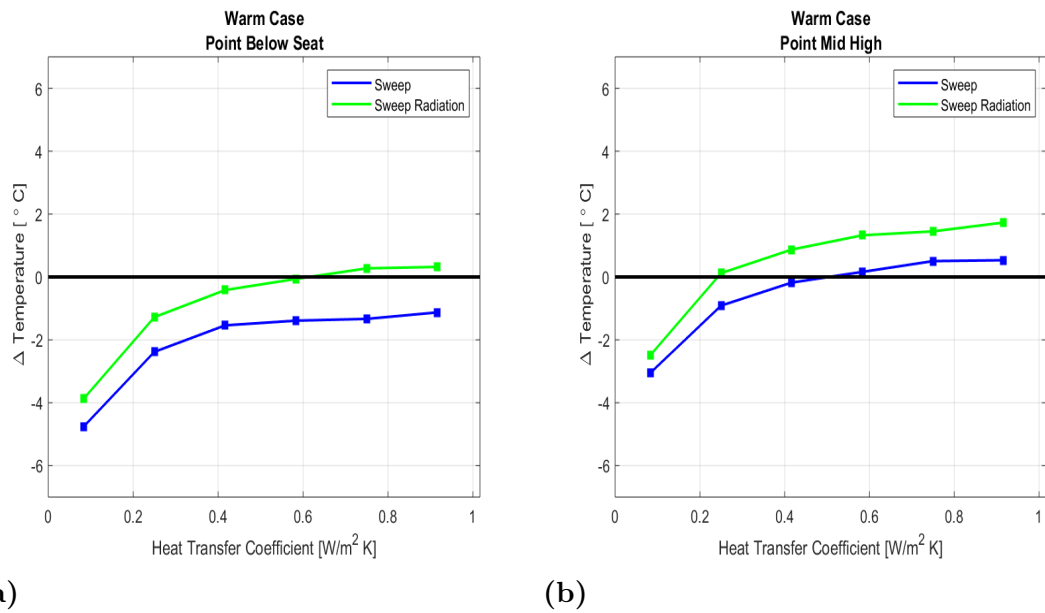


**Figure 4.15:** Warm HTC sweep delta temperatures for points Below Seat and Mid High which are used for computing the set temperature.

The data in Figure 4.15 are used to determine the set temperature of the interior of the bus. The computed set temperature is shown in Figure 4.16a. It can be seen here that the HTC value correspond to the best fit of HTC values in Figure 4.14 and could be a good start for further investigation of other sweeps. Star CCM+ provides other ways to calculate the temperature of the bus. One of these ways is through a volume average of the temperatures in the domain, see Figure 4.16. A volume average calculation of the whole domain is not as dependent on values in single points. It can be seen that this method gives a similar result as the calculated set temperature from the two points in the bus, for this warm case.

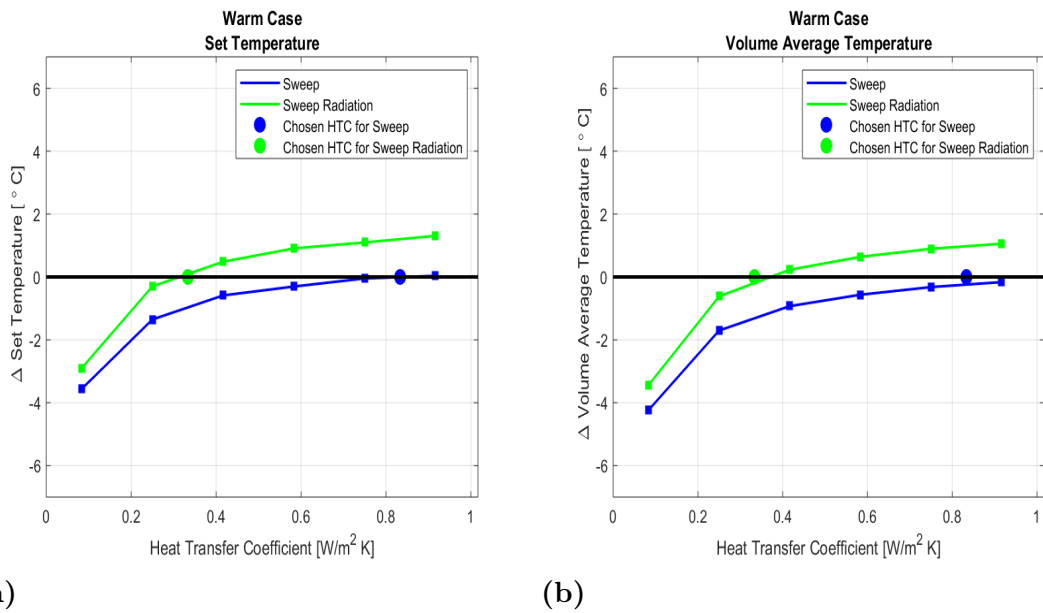


Figure 4.16: Warm HTC sweep set temperature and volume average temperature.

### 4.2.2 Cold case

Results for the HTC sweep of the cold case are presented in this section followed by a discussion of the result's findings. In Figure 4.17-4.19 the temperatures and how they change depending on the value of the HTC is shown. The temperatures are measured at the same positions in the bus as the experimental data. The ambient temperature for the cold case was  $-4.5^{\circ}\text{C}$ .

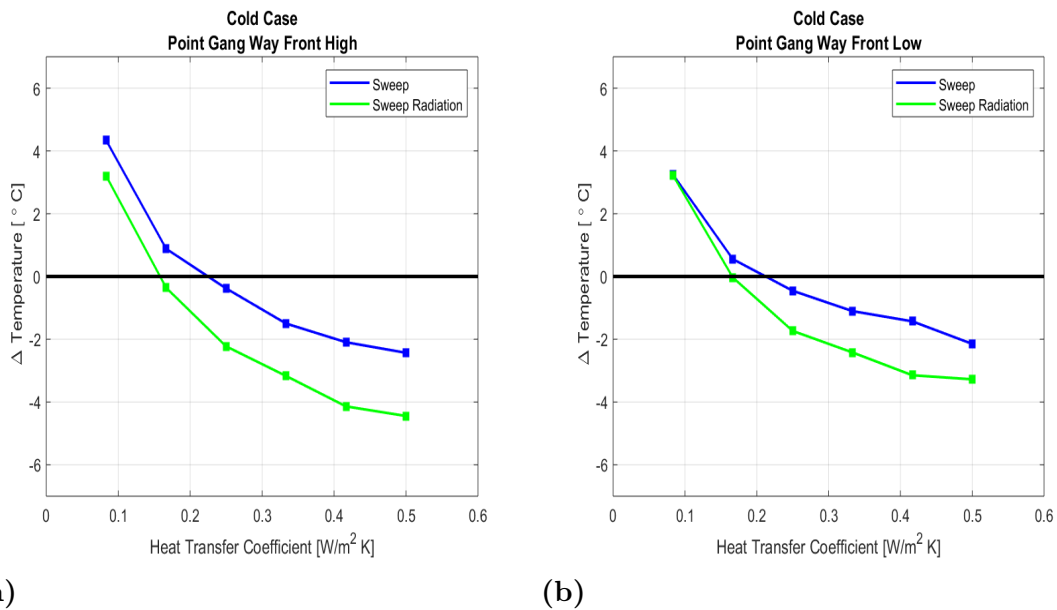
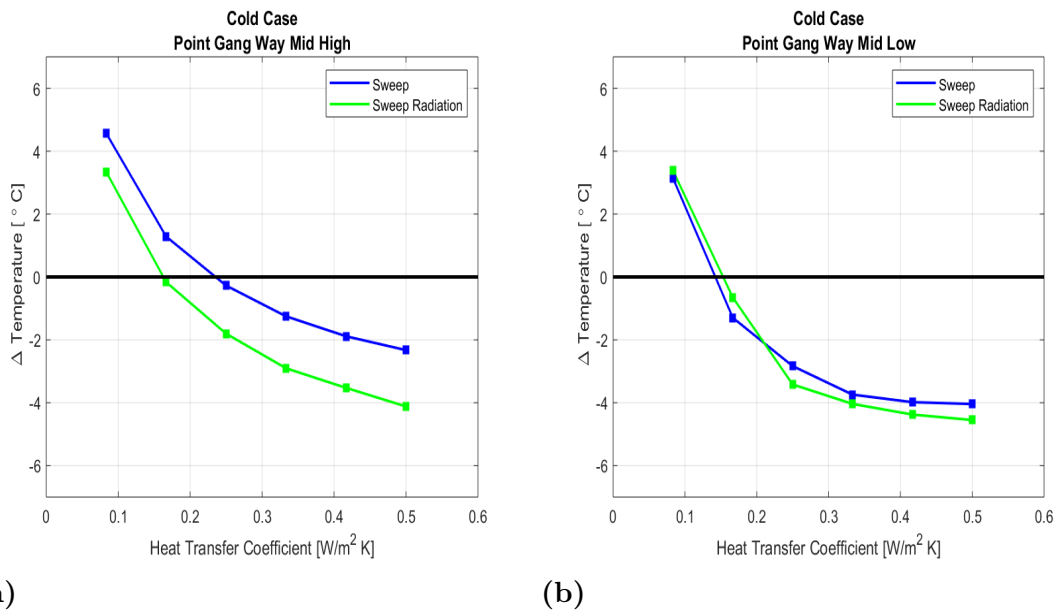
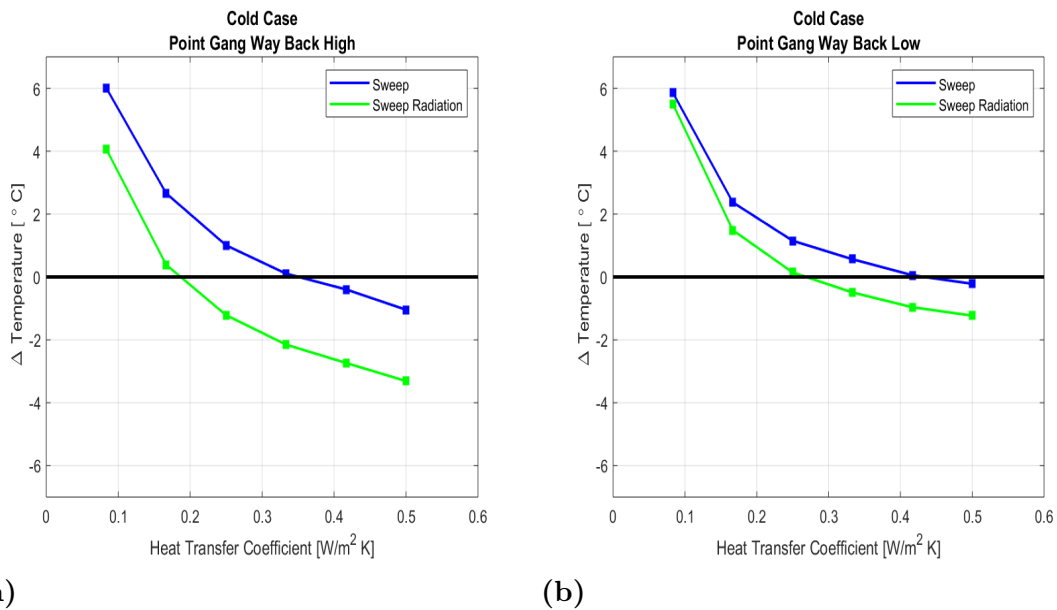


Figure 4.17: Cold HTC sweep delta temperatures for points Gang Way Front High and Low.

## 4. Results and discussion



**Figure 4.18:** Cold HTC sweep delta temperatures for points Gang Way Mid High and Low.



**Figure 4.19:** Cold HTC sweep delta temperatures for points Gang Way Back High and Low.

It can be seen in all graphs above that a higher HTC gives a colder interior. This goes in line with what was described in section 3.5.2 and shows that more convection is captured with higher HTC values.

In general the behaviour in the graphs for the cold case are the same as for the warm case if taking into account that convection is flowing in the other direction. Therefore the graphs have a negative slope in this case instead.

The shape also here is very similar for all the curves both with and without radiation. In these measured points there is also a constant difference in temperature between having radiation active or not.

In Figure 4.20 the average delta temperature of all 6 points presented above is computed. By doing this a best HTC value can be chosen the green and blue round dots in Figure 4.20. All 6 points have been weighted equally.

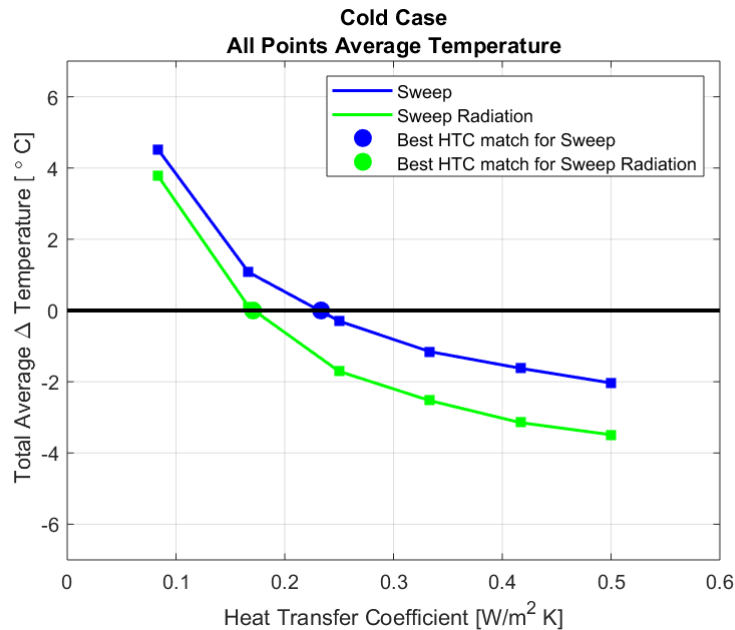


**Figure 4.20:** Average of cold HTC sweep delta temperatures for all points.

By looking at Figure 4.20 the HTC value that gives a best fit with and without radiation can be chosen. This shows that radiation gives an impact on the HTC value even if there is not a significant improvement for the individual points.

## 4. Results and discussion

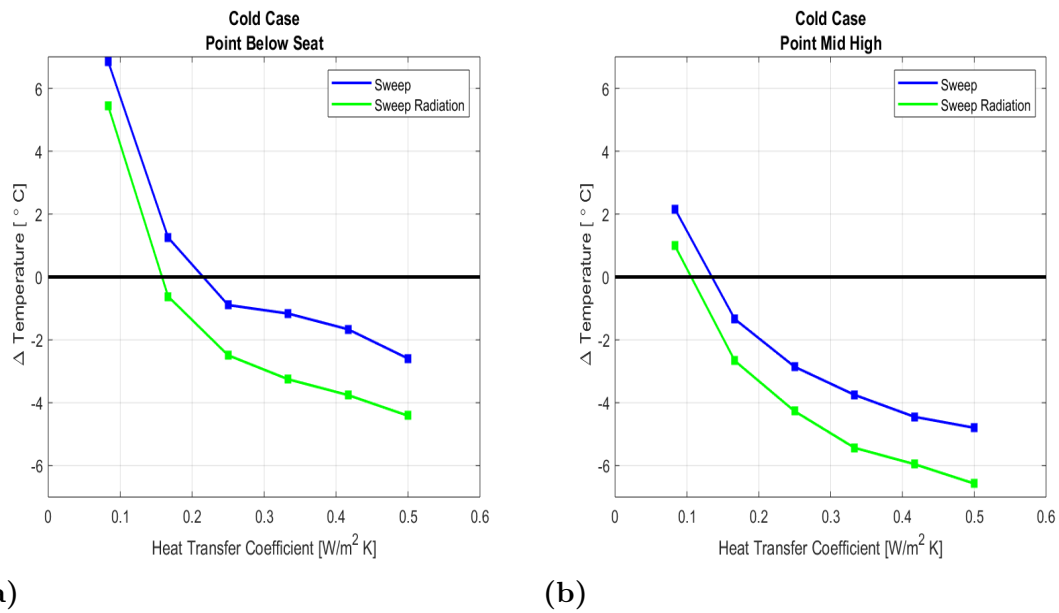


**Figure 4.21:** Cold HTC sweep delta temperatures for points Below Seat and Mid High which are used for computing the set temp.

The data in Figure 4.21 are used to calculate the set temperature of the interior of the bus. The set temperature calculation shown in Figure 4.22a does not match the HTC value from averaging all points as it did in the warm case. Since the temperatures are weighted differently in the set temperature calculation this is nothing strange. It can depend on that the point that is weighted more deviates more from the chosen HTC and therefore the total set temperature also will do that. The volume average temperature in Figure 4.22b that is not depending on the temperature in a specific point matches the HTC values better.

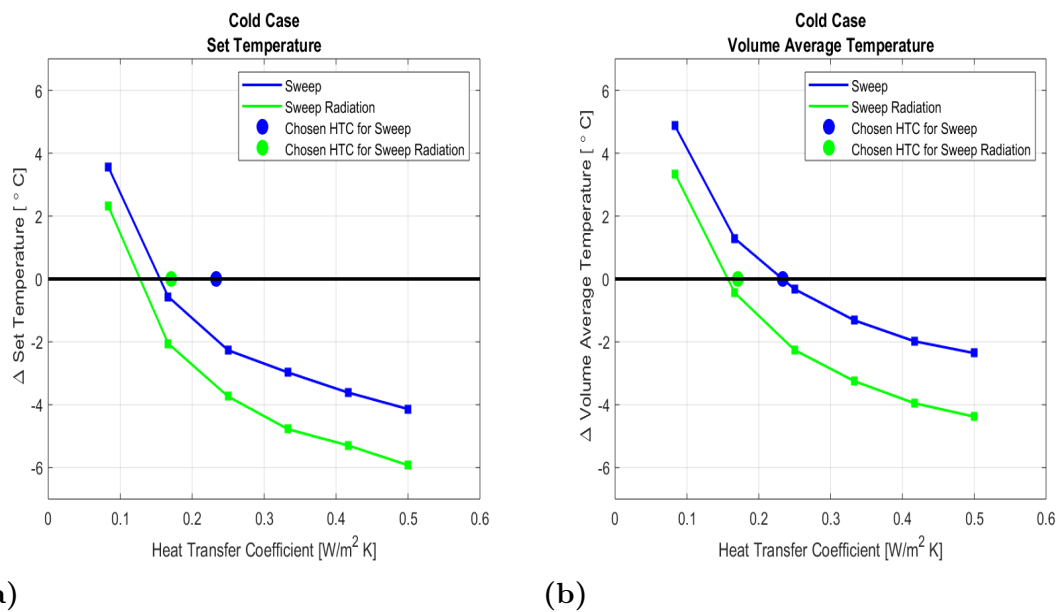


**Figure 4.22:** Cold HTC sweep set temperature and volume average temperature.

### 4.2.3 Comparison between cases results

For the cold case the difference in chosen HTC between the case with radiation and without radiation is less than in the warm case. This might demonstrate that radiation is of greater importance in the warm case than in the cold case. The cold case needs in general a lower HTC than the warm case. This might depend on the difference between ambient temperature and set temperature. For the cold case the delta temperature between set temperature is larger than for the warm case.

If illustrating chosen HTC value vs. ambient temperature for the two cases, as seen in Figure 4.23 it can be seen that the difference between having radiation active or not is larger with higher HTC values, i.e. higher ambient temperature. None of the cases have a perfect match for a single HTC value but a trendline like this could be used to choose an HTC value for cases with ambient temperatures that have not been tested experimentally. The trendline could be used both for interpolating and extrapolating an HTC value for more extreme temperature cases.

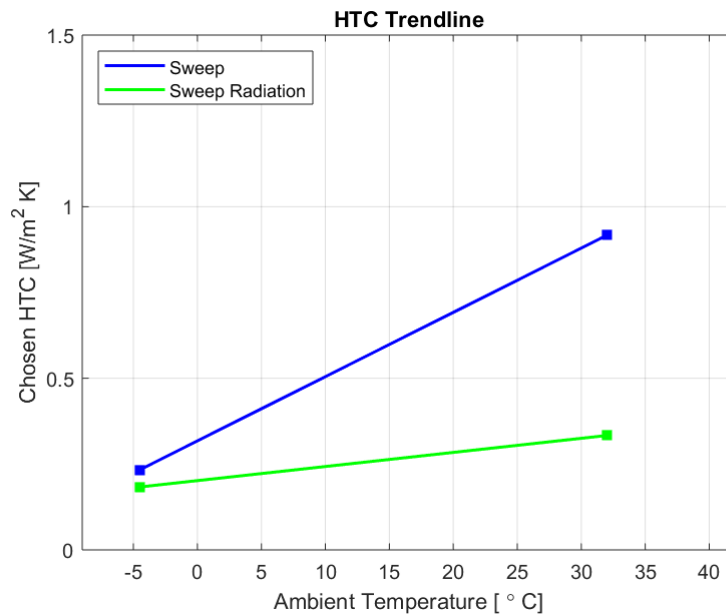


**Figure 4.23:** Best matching HTC values plotted against ambient temperature.



# 5

## Conclusion

In this master thesis a method for simulating steady state interior climate cases for a bus has been produced. In this chapter the most important findings are summarized again.

The major conclusions from the mesh study are the following. It is important to have a mesh with high accuracy through the whole domain. There are equal interest in points close to the surfaces as well as in the rest of the bus since the experimental data is measured at two different heights. It is also important to define a tidy fluid domain with the right usage of surface wrappers. This helps getting rid of unnecessary mesh regions that worsen the stability of the solver. It also helps the work of extracting a detailed enough volume mesh where needed while ensuring a mesh that is not leaking.

For the simulation to converge and work accurately the  $Y+$  values are not allowed to be too high. For the chosen turbulence model the  $Y+$  values should not exceed 100. To avoid this it is important to have small cells on the parts surfaces. In this method prism layers were added to control the  $Y+$  values and resolve boundary layer to simulate convection in a proper way. However the choice of turbulence model may not be the optimal and a further study should be performed.

The main conclusion regarding used boundary conditions is that they are functioning well for steady state cases. Since they have been modelled as black boxes the total energy rates can be controlled but it will not be able to capture time dependent events. The boundary conditions are simplifications of the reality and some details may not be captured. The heat blower's fans are not simulated in detail which may affect the spread of their heat energy.

It was found that buoyancy driven convection is an important solver setting. This is because the fluid is dominated by slow flowing regions and dominated by natural convection. Ideal gas is an important physics model to simulate density variations due to temperature differences. It has also been found that lowering the under-relaxation factors are important for the simulations to be stable and help convergence.

From the HTC sweep the major conclusions were that when simulating warm climate a higher HTC is needed then when simulating cold climate. It was also seen that radiation is more important for warm climate than for cold climate.

The final conclusion is that to be able to calibrate and validate the model more accurately it is important to be part of the planning of the tests. For example the flow fields can be tested experimentally to have more properties to calibrate the model with.

### 5.1 Future Work

As the first step of future work we would recommend an extension of the mesh study focused on prism layers. By lowering  $Y^+$  values more turbulence models could be tried. One problem here was that high  $Y^+$  values were found in the air duct where the cell sizes are already small and the geometry complex. Here it can be difficult to add prism layers so a solution for this must be developed.

A closer study on why ideal gas and constant density models differ should be conducted to decide which one suits this model best. Also the effects of buoyancy should be studied more to get a better understanding of the difference of shear driven and buoyancy driven convection. Another solver setting to study further is the segregated flow solver. According to Siemens Star CCM+ user guide the coupled flow solver is better for varying density and should therefore be tried.

Regarding the HTC sweep the next step could be to have different HTC values on different surfaces. In the developed method all floors, walls, windows and roof are treated in the same way which probably not reflect the reality in a good way. To enable this more preparations of the model has to be done in ANSA. It is important to remember that this will quickly result in more parameters to calibrate which takes computational time. Increasing the numbers of parameters to calibrate increases the number of simulations in a sweep exponentially.

Lastly this method should be extended to transient cases. Transient simulations can be run and calibrated with existing pull-up and pull-down test data. Including transient cases also enables simulating doors being opened and closed.

# Bibliography

- [1] M. Liebers, D.Tretsiak, S.Klement,B. Bäker. et al., “Using Air Walls for the Reduction of Open-Door Heat Losses in Buses,“ SAE Int. J. Commer. Veh. 10(2):2017, doi:10.4271/2017-01-9179.
- [2] K.B. Velt and H.A.M. Daanen, “Optimal bus temperature for thermal comfort during a cool day“, Applied Ergonomics, Volume 62, 2017, Pages 72-76.
- [3] S. Zhu, P. Demokritou, J. Spengler, “Experimental and numerical investigation of micro-environmental conditions in public transportation buses, Building and Environment“, Volume 45, Issue 10, 2010, Pages 2077-2088, ISSN 0360-1323, <https://doi.org/10.1016/j.buildenv.2010.03.004>.
- [4] W. Liu, S. Mazumdar, Z. Zhang, S.B. Poussou, J. Liu, C-H. Lin, Q. Chen, “State-of-the-art methods for studying air distributions in commercial airliner cabins, Building and Environment“, Volume 47, 2012, Pages 5-12, ISSN 0360-1323, <https://doi.org/10.1016/j.buildenv.2011.07.005>.
- [5] C. Suárez, A. Iranzo, J. Salva, E. Tapia, G. Barea, and J. Guerra, “Parametric Investigation Using Computational Fluid Dynamics of the HVAC Air Distribution in a Railway Vehicle for Representative Weather and Operating Conditions,” Energies, vol. 10, no. 8, p. 1074, Jul. 2017.
- [6] UN, *UN Sustainable Development Goals*, <https://www.un.org/sustainabledevelopment/climate-change/> (visited on 2019-05-28)
- [7] L. Davidson, “Fluid mechanics, turbulent flow and turbulence modeling”, Chalmers University of Technology, 2019.
- [8] H.K. Versteeg, and W. Malalasekera, “An introduction to computational fluid dynamics: the finite volume method.” Pearson Prentice Hall, 2007.
- [9] Siemens “Star CCM+ User Guide.“ Version 2019.1
- [10] F.P. Incropera. “Principles of Heat and Mass Transfer.“ 7th ed. Wiley, 2012.
- [11] Arbetsmiljöverket, *Regulations regarding indoor climate* <https://www.av.se/inomhusmiljo/temperatur-och-klimat/> (visited on 2019-05-31)
- [12] Siemens, “The Steve Portal“, *Guidelines for Star CCM+ by Siemens*, <https://thesteveportal.plm.automation.siemens.com/> (visited on 2019-04-15)

